NOTA: anche questa pagina bianca fa parte del blocco di pagine della tesi

NOTA: tagliare il blocco di pagine della tesi (stampata fronte-retro) lungo le due linee qui tracciate prima di effettuare la rilegatura

UNIVERSITÀ DEGLI STUDI DI CATANIA
Dipartimento di Ingegneria Elettrica Elettronica e dei Sistemi

Vincenzo Marletta

FERROELECTRIC E-FIELD SENSORS

A nonlinear dynamic approach to the development of innovative measurement devices

A dissertation submitted in partial fulfillment
of the requirements for the degree of
Doctor of Philosophy
in
Electronic, Automatic and Control of Complex Systems Engineering

Coordinator

Prof. Eng. Luigi Fortuna

Tutor

Prof. Eng. Salvatore Baglio

Co-tutor

Prof. Eng. Bruno Andò

Academic Year 2009-10

ABSTRACT

The exploitation of nonlinear dynamics behavior in ferroelectric material toward the realization of innovative transducers for the detection of weak and low frequency electric fields is the focus of this thesis.
A nonlinear dynamical system based on ferroelectric capacitors coupled into a unidirectional ring circuit is considered with particular interest for developing novel electric field sensors.
The focused approach is based on the exploitation of circuits made up by the ring connection of an odd number of elements containing a ferroelectric capacitor, which under particular conditions exhibits an oscillating regime of behavior. For such a device a weak, external, target electric field interacts with the system thus inducing perturbation of the polarization of the ferroelectric material; this, the target signal can be indirectly detected and quantified via its effect on the system response.
The conceived devices exploit the synergetic use of bi-stable ferroelectric materials, micromachining technologies that allow us to address charge density amplification, and implement novel sensing strategies based on coupling non-linear elemental cells.
Advanced simulation tools have been used for modeling a system including electronic components and non linear elements as the conceived micro-capacitors. Moreover, Finite Element Analysis (FEM) has allowed us to steer the capacitor electrodes design toward optimal geometries and to improve the knowledge of effects of the external target E-field on the electric potential acting on the ferroelectric material.
An experimental characterization of the whole circuit, including three cells coupled in a ring configuration has also been carried out.

ACKNOWLEDGEMENTS

I want to take this opportunity to thank all the people who directly and indirectly have helped me and who continue to inspire me.
My supervisor, Salvatore Baglio who believed in me and gave me the chance to follow the PhD program in the electrical and electronic measurements group about the things that I have always been interested in: the fascinating world of sensors. He taught me to never stop facing the difficulties and occasionally blamed me pointing me in the right direction. I hope that the way in which I worked was to his liking. For my part I have always had the goal to prove that I can do. Especially I always worked thinking that the little that I was doing was research and science, and then everything had to be explained and that anyone who had seen or read my work had to be convinced of its validity not as an act of faith but because there were experimental evidences.
I am really grateful to my co-supervisor Bruno Andò, whose door was always open for me whenever I needed guidance and with great patience has always had an advice and something to teach me. Your suggestions and explanations has been valuable.
I want to thank the coordinator, Prof. Luigi Fortuna who always is working to enhance the quality of this PhD course despite the financial difficulties facing the universities.
To all my colleagues I have met in these three years at the laboratory of Electric and Electronic Measurements (in no particular order and I am sorry if I forgot someone): Salvatore Strazzeri, Alberto Ascia, Carlo Trigona, Nicolò Savalli, Paola Brunetto, Salvatore La Malfa, Angela Beninato, Francesco Pagano and Elena Umana, thank you! It was a pleasure to know you and I had a lot of good time with you. I wish you all the best for your future, wherever it will lead you. Hopefully we see us again sometimes - somewhere.

ACKNOWLEDGEMENTS

In these three years I have met a lot of people, many of them were recognized scientists. I want to thank Dr. Adi R. Bulsara of the Space and Naval Warfare Systems Center (SPAWAR) in San Diego (CA, USA) who has provided funds for this research. In addition to being an internationally recognized scientist is also a nice person and a hearty eater who love our food.
I also want to thank Dr. Antonio La Mantia and his staff at ST Microelectronics of Catania for his courtesy and collaboration and to gave us the possibility to use the FIB in his laboratory to work on our capacitors.
Despite I have not ever met him I want to thank Dr. Joe Evans of Radiant Technologies Inc. in Albuquerque(NM, USA) for his continuous support in designing our ferroelectric capacitors.
Last but not least important I need to thank my wife, Silvia. She patiently endured my late nights and odd hours, comforted me when I was down and always supported me understanding that I loved my work. I'm sorry for every Sunday you've been alone because I was locked up in the next room to work. I hope to recover it.
I love you and cannot thank you sufficiently enough. This thesis is dedicated to you!

Many thanks to all of you!

Vincenzo Marletta

December 5th, 2010

To my wife Silvia

CONTENTS

LIST OF FIGURES

CHAPTER 2

CHAPTER 3

CHAPTER 4

APPENDIX

LIST OF TABLES

CHAPTER 2

CHAPTER 3

CHAPTER 4

CHAPTER 1

INTRODUCTION

An experiment is a question which science poses to Nature, and a measurement is the recording of Nature's answer.
- Max Planck

You make experiments and I make theories. Do you know the difference? A theory is something nobody believes, except the person who made it. An experiment is something everybody believes, except the person who made it.
- Albert Einstein

Ferroelectric materials are defined as those which exhibit, at temperatures below the Curie point, a domain structure and spontaneous polarization which can be reoriented by applied electric fields. The domain morphology results from the alignment of dipoles to minimize electrostatic and elastic energy, and materials with this structure will exhibit varying degrees of hysteresis at all drive levels.

Research and development in ferroelectric materials has advanced at an unimaginable rate in the past decade, driven mainly by three factors: new forms of materials, prepared in a multitude of sizes [1] (e.g. bulk single crystals and ceramics, nano-structured films, tubes, wires and particles) by a variety of techniques [2] (e.g. melt growth, physical

deposition and to soft chemical synthesis); novel and intricate structural and physical properties have been discovered in these materials [2] (e.g. morphotropic phase boundary and related phenomena, domain engineering under fields, effects of nanostructures and superlattices); and the extraordinary potential offered by these materials to be used in the fabrication of a wide range of high-performance devices [3] (such as sensors, actuators, medical ultrasonic transducers, micro electromechanical systems (MEMS), microwave tuners, ferroelectric non-volatile random access memories (FeRAM), electro-optical modulators, etc.).

Ferroelectrics can be utilized in various devices such as high-permittivity dielectrics, pyroelectric sensor, piezoelectric devices, electrooptic devices and PTC components. The industries are producing large amounts of simple devices, e.g. ceramic capacitors, piezoelectric igniters, buzzers and PTC thermistors continuously [3]. But until now ferroelectric devices have failed to reach commercialization in more functional cases. In the light sensor, for example, semiconductive materials are superior to ferroelectrics in response speed and sensitivity. Magnetic devices are much more popular in the memory field, and liquid crystals are typically used for optical displays.

Starting from these considerations and taking in account the solid background on nonlinear dynamical systems at DIEES of the University of Catania, a nonlinear dynamical system based on ferroelectric capacitors coupled into a unidirectional ring circuit is considered with particular interest for developing novel electric field sensors.

This thesis deals with the exploitation of ferroelectric material properties and nonlinear dynamics behavior with emphasis on the realization of an innovative transducer.

The focused approach is based on the exploitation of circuits made up by the ring connection of an odd number of elements containing a ferroelectric capacitor, which under particular conditions exhibits an oscillating regime of behavior. For such a device, an external target electric field interacts with the system thus inducing perturbation of the polarization of the ferroelectric material; this, the target signal can be indirectly detected and quantified via its effect on the system response.

The research work carried out for this Ph.D. thesis has been divided in five chapters, including this introduction, as summarized below briefly:

CHAPTER 2 is divided into two main sections: in the first section physical notions about electric fields and dielectric materials are given while in the second section a review of traditional instrumentation to measure electric fields together with a state of art on E-field sensors applications is presented.

CHAPTER 3 deals with ferroelectric materials: starting with an historical introduction to ferroelectrics, some theoretical notions together with a review of more popular ferroelectric material is given. The chapter ends with a state of art on ferroelectrics applications.

CHAPTER 4 reports both theoretical and experimental results. The theory underpinning the system investigated here is presented together with simulations and experimental results.

CHAPTER 5 concludes this thesis.

CHAPTER 2

ELECTRIC FIELD BASES AND INSTRUMENTATION

The important thing is to know how to take all things quietly.
- Michael Faraday

1. ELECTRIC FIELD BASES

1.1. ELECTRIC FIELD

The concept of an electric field (E-field) was introduced by Michael Faraday in nineteenth century to address a property that describes the space that surrounds electrically charged particles as shown in Figure 2-1 or that which is in the presence of a time-varying magnetic field.

The electric field is a vector field with SI units of Newtons per Coulomb (NC^{-1}) or, equivalently, Volts per meter (Vm^{-1}). The strength E of the field at a given point is defined as the force F that would be exerted on a positive test charge q of 1 coulomb placed at that point; the direction of the field is given by the direction of that force

$$\vec{E} = \frac{\vec{F}}{q} \quad \left[\frac{N}{C}\right] \tag{2.1}$$

This electric field exerts a force on other electrically charged objects.

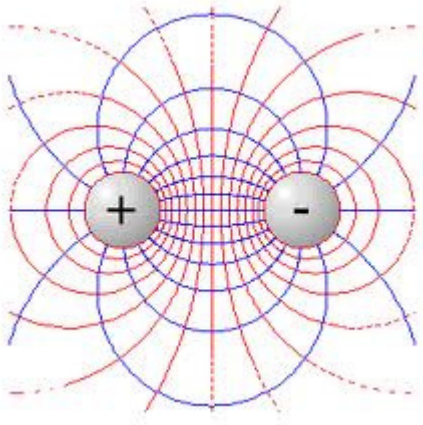

FIGURE 2-1 The electric field surrounding a positive and a negative charge.

The direction of the electric field is the same as the direction of the force it would exert on a positively-charged particle, and opposite the direction of the force on a negatively-charged particle.
Since like charges repel and opposites attract, the electric field tends to point away from positive charges and towards negative charges.
The fundamental equation which describes the force between two point charges is Coulomb's law [4]. The magnitude of the electrostatic force between two point electric charges Q_1 and Q_2 is directly proportional to the product of the magnitudes of each charge and inversely proportional to the square of the distance between the charges

$$F = \frac{Q_1 Q_2}{4\pi\varepsilon_0 r^2} \quad [N] \tag{2.2}$$

where ε_0 is a constant called the permittivity of free space, defined as

$$\varepsilon_0 \equiv \frac{1}{\mu_0 c_0^2} \approx 8.854187817\times10^{-12} \quad \left[\frac{F}{m}\right] \tag{2.3}$$

where c_0 is the speed of light in free space while μ_0 is the vacuum permeability.

Based on Coulomb's law for interacting point charges, the contribution to the E-field at a point in space due to a single, discrete charge located at another point in space is given by the following

$$E = \frac{1}{4\pi\varepsilon_0}\frac{q}{r^2}\hat{r} \tag{2.4}$$

where q is the charge of the particle creating the electric force, r is the distance from the particle with charge q to the E-field evaluation point, $\hat{r}$ is the unit vector pointing from the particle with charge q to the E-field evaluation point, ε_0 is the permittivity.

The total E-field due to a quantity of point charges n_q, is simply the superposition of the contribution of each individual point charge

$$E = \sum_{i=1}^{n_q} E_i = \sum_{i=1}^{n_q} \frac{1}{4\pi\varepsilon_0}\frac{q_i}{r_i^2}\hat{r}_i \tag{2.5}$$

Alternately, Gauss's law allows the E-field to be calculated in terms of a continuous distribution of charge density in space ρ

$$\nabla \cdot E = \frac{\rho}{\varepsilon_0} \tag{2.6}$$

where the symbol ∇ is used to represent the *del* operator (see section 3). Coulomb's law is actually a special case of Gauss's law, a more fundamental description of the relationship between the distribution of electric charge in space and the resulting electric field [4]. Gauss's law is one of Maxwell's equations, a set of four laws governing electromagnetic.

Electric fields contain electrical energy with energy density proportional to the square of the field amplitude

$$u = \frac{1}{2}\varepsilon|E|^2 \tag{2.7}$$

where ε is the permittivity of the medium in which the field exists, and E is the electric field vector. The total energy stored in the electric field in a given volume V is therefore

$$\frac{1}{2}\varepsilon\int_V |E|^2 dV \tag{2.8}$$

where dV is the differential volume element.
An electric field that changes with time (such as due to the motion of charged particles in the field) will also influence the magnetic field of that region of space. As they move, they generate magnetic fields, and if the magnetic field changes, it generates electric fields (see section 9). A changing magnetic field gives rise to an electric field

$$E = -\nabla V - \frac{\partial A}{\partial t} \tag{2.9}$$

which yields Faraday's law of induction

$$\nabla \times E = -\frac{\partial B}{\partial t} \tag{2.10}$$

where $\nabla \times E$ indicates the curl (or rotor) of the electric field. For more details see section 10.
This means that a magnetic field changing in time produces a curled electric field, possibly also changing in time. The situation in which electric or magnetic fields change in time is no longer electrostatics, but rather electrodynamics or electromagnetics.
Thus, in general, the electric and magnetic fields are not completely separate phenomenon. For this reason, one speaks of "electromagnetism" or "electromagnetic fields".

1.2. ELECTRIC WORK AND VOLTAGE

Relationship (2.1) is valid when the electric charges creating the electric field are fixed and constant in time and the charge q on which the E-field exerts the force is also fixed or movable without perturbing the electric charges distribution [4].
The work of the force F on a displacement ds of the charge q is given by

$$dW = F \cdot ds = q\,E \cdot ds = q\,E\cos\theta ds \tag{2.11}$$

where θ is the angle between the electric field E and the displacement ds. For a displacement from a position A to a position B over a path C_1 the electric work is given by

$$W = \int_{C_1} dW = \int_{C_1} F \cdot ds = q\int_{C_1} E \cdot ds \tag{2.12}$$

The last integral in (2.12), that is the ratio between the electric force and the charge is the line integral of the electric field E over the path C_1 and defines the electric voltage between the two points A and B related to the path C_1. Choosing another path C_2 from the same points A and B we will find a different electric work then a different value of the electric voltage.

For a closed path C constituted, for example, by the path C_1 from A to B and by the path C_2 from B to A the work results to be

$$W = \oint_C F \cdot ds = \int_{C_1} F \cdot ds + \int_{-C_2} F \cdot ds = \int_{C_1} F \cdot ds - \int_{C_2} F \cdot ds = W_1 - W_2 \tag{2.13}$$

which in general is not zero. Taking in account the (2.1)

$$W = \oint_C F \cdot ds = q\oint_C E \cdot ds = q\xi \tag{2.14}$$

where ξ is the electromotive force.

Not any electric force is conservative but this is the case of the electrostatic forces for which the (2.12) can be rewritten in terms of the difference of the values of a function of the coordinates

$$\int_A^B E \cdot ds = f(B) - f(A) \tag{2.15}$$

The opposite of this function is named potential difference between the points A and B

$$V_A - V_B = \int_A^B E \cdot ds \tag{2.16}$$

From relationships (2.14) and (2.16) it follows that for a closed path in the space where the electric field E is defined

$$\xi = \oint E \cdot ds = 0 \quad , \quad W = qE = 0 \tag{2.17}$$

1.3. THE E-FIELD AS POTENTIAL GRADIENT

The potential is a continues scalar function and derivable. For a displacement $dr = dx\,u_x + dy\,u_y + dz\,u_z$ from a point $A(x, y, z)$ to $B(x+dx, y+dy, z+dz)$ the potential variation is

$$dV = V(x+dx, y+dy, z+dz) - V(x, y, z) = -E \cdot dr = -E_x dx - E_y dy - E_z dz$$

On the other hand for the total differential theorem

$$dV = \frac{\partial V}{\partial x} dx + \frac{\partial V}{\partial y} dy + \frac{\partial V}{\partial z} dz \tag{2.18}$$

and from the comparison of this last two equations it follows that

$$E_x = -\frac{\partial V}{\partial x} \quad , \quad E_y = -\frac{\partial V}{\partial y} \quad , \quad E_z = -\frac{\partial V}{\partial z} \tag{2.19}$$

which can be synthetically written as

$$E = -grad\ V \tag{2.20}$$

or altenatively, introducing the *del* operator

$$\nabla = \frac{\partial}{\partial x} u_x + \frac{\partial}{\partial y} u_y + \frac{\partial}{\partial z} u_z \tag{2.21}$$

as it follows

$$E = -grad\ V = -\nabla V \tag{2.22}$$

As a consequence the (2.16) can be rewritten as

$$V_A - V_B = \int_A^B E \cdot ds = -\int_A^B \nabla V \cdot ds \tag{2.23}$$

1.4. CAPACITY OF AN ISOLATED CONDUCTOR

The electric charge distributed on the surface Σ of a conductor far from other charged bodies is related to the surface density σ by the equation

$$q = \oint \sigma(x', y', z')\, d\Sigma \tag{2.24}$$

Under the electrostatic conditions all the electric charges are fixed then inside the conductor the electric field is null. One important consequence of this condition is that the potential is constant in every point of the conductor: given two any points P_1 and P_2

$$V(P_1) - V(P_2) = \int_{P_1}^{P_2} E \cdot ds = 0 \quad \Rightarrow \quad V(P_1) = V(P_2) = V_0 \quad (2.25)$$

therefore the surface of the conductor is equipotential. Moreover the charge distribution assuring this condition is one and only one [4].
If the charge q is changed to the value $q' = mq$ also the density and the potential changes of the same quantity. It follows that the ratio between the charge and the potential of the isolated conductor does not changes as the charge changes

$$C = \frac{q}{V} \quad (2.26)$$

this ratio is named capacity and depends only from the shape and the dimensions of the conductor and from the properties of the surrounding medium. The unit of measurement of the capacity is coulomb/volt also named farad whose symbol is F.
This equation is valid for every couple of conductors for which there is a complete induction; such a system is called capacitor and the two conductors are named armors. The ratio between the absolute value of the charge on one of the armors and the potential difference is called capacity of the capacitor

$$C = \frac{q}{V_1 - V_2} \quad (2.27)$$

The capacity depends on the geometry of the armors and on the properties of the interposed medium.

1.5. CONNECTION OF CAPACITORS

A capacitor is essentially used to store electric charges; although the total charge is null it is separated in the two quantities $+q$ and $-q$ which

for a capacitor are proportional to the potential difference between the armors. By suitable external conductive links it is possible to flow the negative charge from an armor to the other one so generating an electric current which discharges the capacitor.
In the following the configurations of connection of capacitors are faced together with the evaluation of the equivalent total capacity. The charges and the potential differences will be supposed to be constant in time but the results are valid even for variable quantities.
For the sake of convenience we will indicate with V the potential difference V_1-V_2 between the armors and with C both the capacitor and its capacitance. The circuital symbol of a capacitor (regardless of the geometry of its armors) is shown in Figure 2-2a.

Capacitors in series

The schematic of the connection in series is shown in Figure 2-2b. Every capacitor is connected to the next by only one link: the potential difference V is applied to the extremes of the series. Due to the induction effect the charge in every capacitor of the series is the same

$$V_1 = \frac{q}{C_1}, \quad V_2 = \frac{q}{C_2}, \quad \cdots \quad V_n = \frac{q}{C_n} \tag{2.28}$$

The total potential difference is given by the sum of the potential difference of every single capacitor

$$V = V_1 + V_2 + \cdots + V_n = \frac{q}{C_1} + \frac{q}{C_2} + \cdots + \frac{q}{C_n} = q\left(\frac{1}{C_1} + \frac{1}{C_2} + \cdots + \frac{1}{C_n}\right) = \frac{q}{C_{eq}} \tag{2.29}$$

where

$$\frac{1}{C_{eq}} = \frac{1}{C_1} + \frac{1}{C_2} + \cdots + \frac{1}{C_n}, \quad C_{eq} = \frac{C_1 C_2 \cdots C_n}{C_1 + C_2 + \cdots + C_n} \tag{2.30}$$

The inverse of the equivalent capacitance of the series is the sum of the inverse of the capacitance of the singles capacitors.

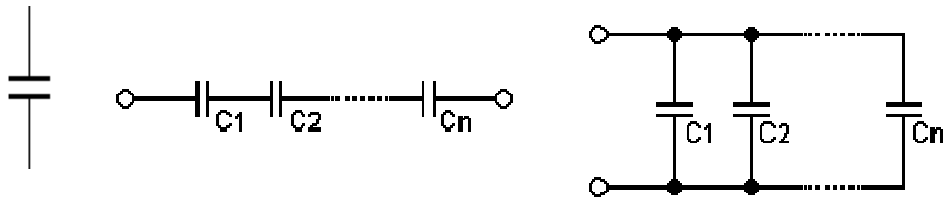

(a) (b) (c)

FIGURE 2-1 Connection of capacitors. (a) The circuital symbol of a capacitor; (b) Capacitors in series; (c) Capacitors in parallel.

Capacitors in parallel

The schematic of the connection in parallel is shown in Figure 2-2c. Every capacitor is connected to the next by both the two armors: the same potential difference V is applied to the armors of every single capacitor

$$q_1 = C_1 V \ , \ q_2 = C_2 V \ , \cdots , \ q_n = C_n V \tag{2.31}$$

the total charge of the system is given by the sum of the charges of every single capacitor

$$q = q_1 + q_2 + \cdots + q_n = (C_1 + C_2 + \cdots + C_n)V = C_{eq} V \tag{2.32}$$

The equivalent capacitance of the parallel is then the sum of the capacitance of the singles capacitors.

1.6. DIELECTRICS. THE DIELECTRIC CONSTANT

Let to consider a charged and isolated parallel plates capacitor: the charge q_0 distributed uniformly with density σ_0 produces, between the armors, an electric field and a potential difference given by

$$E_0 = \frac{\sigma_0}{\varepsilon_0} \quad , \quad V_0 = \frac{q_0}{C_0} = E_0 h \tag{2.33}$$

where C_0 is the capacitance and h the distance between the armors.
Imagine to insert a conductive plate with thickness $s<h$ among the armors without touching them: the potential difference between the

armors decreases due to the electrostatic induction on both the faces of the plate of a density distribution σ_0 with opposite sign to null the field inside the plate; outside the field does not change then

$$V = E_0(h - s) < V_0 \tag{2.34}$$

Repeating the experiment with an insulating material with the same thickness the potential difference decreases less than in the previous case. The potential difference decreases linearly with increasing of the thickness of the plate assuming the least value V_k when the insulating material totally fills the space between the armors.

Faraday has demonstrated that the ratio between the potential difference V_0 without insulating material and the least value of the potential difference V_k is always greater than 1 depending only by the material properties. The insulating materials having the property to reduce the potential difference between the armors and then the electric field are called dielectrics and the dimensionless ratio [4]

$$\kappa = \frac{V_0}{V_k} > 1 \tag{2.35}$$

is named relative dielectric constant.

For the capacitor filled by the insulating the electric field is

$$E_k = \frac{V_k}{h} = \frac{V_0}{\kappa h} = \frac{E_0}{\kappa} = \frac{\sigma_0}{\kappa \varepsilon_0} \tag{2.36}$$

then reduced by the factor κ. The variation of the electric field due to the dielectric is

$$E_0 - E_k = \frac{\sigma_0}{\varepsilon_0} - \frac{\sigma_0}{\kappa \varepsilon_0} = \frac{\kappa - 1}{\kappa} \frac{\sigma_0}{\varepsilon_0} = \frac{\chi}{1 + \chi} \frac{\sigma_0}{\varepsilon_0} \tag{2.37}$$

where $\chi = \kappa - 1$ is the electric suscettivity of the dielectric.

The capacitance is

$$C_k = \frac{q_0}{V_k} = \kappa \frac{q_0}{V_0} = \kappa C_0 \tag{2.38}$$

that is the capacitance of the capacitor fulfilled by an insulating is increased by the factor κ.

1.7. DIELECTRICS POLARIZATION

In absence of an electric field the electrons of an atom are on average distributed symmetrically around the nucleus: it is represented as a negative charged cloud filling a region around the nucleus with a radius equal to the atom dimension (~10^{-10} m); the center of mass of the negative cloud coincides with positive nucleus.
Under the effect of an E-field the center of mass of the negative cloud is moved in the opposite direction of the field while the positive nucleus is moved in the same direction of the field; an equilibrium position is reached when this effect is balanced by the attraction forces of the opposite charges. Named x the vector going from the centre of the negative charge to the nucleus the electric dipole moment can be defined as it follows

$$p_a = Zex \tag{2.39}$$

where Z is the atomic number and e the charge of the electron. The phenomenon is called electronic polarization and vanishes when the E-field is annulled. Every atom gains a mean electric dipole moment $<p>$ parallel and having the same direction of the E-field.
Considering a volume $\Delta\tau$ containing ΔN atoms, the resulting dipole moment is $\Delta p = \Delta N < p >$ and the dipole moment per unit of volume is

$$P = \frac{\Delta p}{\Delta \tau} = \frac{\Delta N}{\Delta \tau} < p >= n < p > \tag{2.40}$$

where n is the number of atoms per unit of volume. The vector P is called polarization of the dielectric. In most dielectrics P results to be proportional to the E-field according to the following relation [4]

$$P = \varepsilon_0(\kappa - 1)E = \varepsilon_0 \chi E \tag{2.41}$$

Dielectrics obeying the rule (2.41) are called linear and are amorphous and isotropic materials.

The electric field generated by static charges remains to be conservative even with polarized dielectrics. Also the Gauss's law is valid provided that the charges due to the polarization are taken into account

$$\nabla \cdot E = \frac{\rho + \rho_p}{\varepsilon_0} \tag{2.42}$$

these charges are not free to move and are distributed with density

$$\rho_p = \frac{dq_p}{d\tau} = -\nabla \cdot P \tag{2.43}$$

then from the (2.42) it results

$$\varepsilon_0 \nabla \cdot E = \nabla \cdot \varepsilon_0 E = \rho - \nabla \cdot P \Rightarrow \nabla \cdot \left(\varepsilon_0 E + P\right) = \rho \tag{2.44}$$

Introducing the dielectric induction vector D

$$D = \varepsilon_0 E + P \tag{2.45}$$

it follows

$$\nabla \cdot D = \rho \tag{2.46}$$

it depends only from the free charges, if no free charges are present $\nabla \cdot D = 0$ then vector field D is solenoidal, moreover it is not conservative [4].
The polarization and the dielectric induction have the same unit of measurement that is that of the surface density of charge C/m^2.

1.8. ISOTROPIC AND ANISOTROPIC DIELECTRICS

From equation (2.41) and taking in account (2.45) it follows

$$D = \varepsilon_0 E + P = \varepsilon_0 (1 + \chi) E = \varepsilon_0 \kappa E = \varepsilon E \tag{2.47}$$

where ε is the absolute dielectric constant; and using (2.47) in (2.41) $P = \varepsilon_0 (\kappa - 1) D / \varepsilon$ that is

$$P = \frac{\kappa - 1}{\kappa} D = \frac{\chi}{1 + \chi} D \tag{2.48}$$

In a linear (then isotropic) dielectric the dielectric induction, the electric field and the polarization are vectors parallel to each other [4].
If the linear dielectric is homogeneous, that is the density is constant, even the relative dielectric constant is constant everywhere and from (2.48) it follows

$$\nabla \cdot P = \frac{\kappa - 1}{\kappa} \nabla \cdot D \tag{2.49}$$

since in the dielectric there are not free charge $\nabla \cdot D = 0$ then

$$\rho_p = -\nabla \cdot P = 0 \tag{2.50}$$

In a homogeneous linear dielectric the spatial density of polarization charge is null and the polarization charges are distributed only on the surface [4].
When the relative dielectric constant is not constant and changes from point to point, from (2.49) it follows

$$\nabla \cdot P = \frac{\kappa - 1}{\kappa} \nabla \cdot D + D \cdot \nabla \left(\frac{\kappa - 1}{\kappa} \right) \tag{2.51}$$

Even if there are not free charges in the dielectric the divergence of P is not zero and depends on the gradient of function $(\kappa - 1)/\kappa$

$$\rho_p = -\nabla \cdot P = -D \cdot \nabla \left(\frac{\kappa - 1}{\kappa} \right) \tag{2.52}$$

For the anisotropic dielectric like crystals, generally the polarization P is not parallel to the electric field E and the relation between this two quantity is given by the following triad

$$\begin{aligned} P_x &= \varepsilon_0 \left(\chi_{11} E_x + \chi_{12} E_y + \chi_{13} E_z \right) \\ P_y &= \varepsilon_0 \left(\chi_{21} E_x + \chi_{22} E_y + \chi_{23} E_z \right) \\ P_z &= \varepsilon_0 \left(\chi_{31} E_x + \chi_{32} E_y + \chi_{33} E_z \right) \end{aligned} \tag{2.53}$$

The nine numbers χ_{ij} constitute the electric suscettivity tensor; actually they are six because $\chi_{ij} = \chi_{ji} \; (i \neq j)$ that is the tensor is symmetric [4].

Not even the vector D is parallel to the field E. However in these materials there three characteristic directions named crystallographic axes or optical axes of the dielectric which are mutually orthogonal and along which E, P and D are parallel.

1.9. TIME-VARIABLE ELECTRIC AND MAGNETIC FIELDS

The local properties of time-constant electric fields E and magnetic fields B are determined in the vacuum by the four Maxwell's equations

$$\begin{aligned} \nabla \cdot E &= \frac{\rho}{\varepsilon_0} \quad , \quad \nabla \times E = 0 \\ \nabla \cdot B &= 0 \quad , \quad \nabla \times B = \mu_0 j \end{aligned} \tag{2.54}$$

where the sources are represented by the charge density $\rho(x, y, z)$ and the current density $j(x, y, z)$ both constant in time. The steady state condition is underlined by the fact that in (2.54) do not compare the time derivation.

The static and conservative E-field is generated by the fixed electric charges while the static magnetic field is generated by the electric charges in steady movement. Except that the sources of the static fields are the electric charges there is not any other relation between static electric and magnetic phenomenon.

A different relation between electricity and magnetism has been highlighted by Faraday and (separately) Henry's experiments: a time-variable magnetic field produces a not conservative electric field which in suitable devices can generate an electromotive force or a current in a closed circuit; the same effect can be highlighted when a circuit moves respect a constant magnetic field. Subsequently Maxwell have demonstrated that a time-variable electric field generates a magnetic field reaching a more general form of the equations regulating the variable electric and magnetic phenomenon having the (2.54) as the particular static case. The fundamental results is that variables electric and magnetic fields can't exist separately but have to be bring together under the more general concept of the electromagnetic field.

1.10. FARADAY'S LAW

Experiments conducted by Faraday have demonstrated that whenever the flux of the magnetic field $\Phi(B)$ concatenated with a circuit changes in time it induces in the circuit an electromotive force given by

$$\xi_i = -\frac{d\Phi(B)}{dt} \tag{2.55}$$

that is called Faraday's law of the electromagnetic induction. The effect of the induced electromotive force is such to oppose to the generating phenomenon, this statement is known as Lenz's law [4].
By the definition of electromotive force and magnetic flux it follows

$$\xi_i = \oint E_i \cdot ds = -\frac{d\Phi(B)}{dt} = -\frac{d}{dt}\int_\Sigma B \cdot u_n d\Sigma \tag{2.56}$$

the variation of the magnetic flux concatenated with a closed path s generates an induced electric field E_i whose circuitation along s is $-d\Phi/dt$. Then this field is not conservative. Σ is a surface having s as edge.
The variation of the flux can be generated in different ways that can be classified in two main causes: the motion of a conductor in a reference system where the sources of the magnetic field are fixed and the time-variation of the magnetic field in a reference system in which the conductor is fixed. Focusing at this latter case let to reconsider the (2.56) moving the time derivation under the integration

$$\xi_i = \oint E \cdot ds = -\int_\Sigma \frac{\partial B}{\partial t} \cdot u_n d\Sigma \tag{2.57}$$

Applying the Stokes's theorem

$$\oint E \cdot ds = \int_\Sigma \nabla \times E \cdot u_n \, d\Sigma = -\int_\Sigma \frac{\partial B}{\partial t} \cdot u_n \, d\Sigma \tag{2.58}$$

from which it follows that

$$\nabla \times E = -\frac{\partial B}{\partial t} \tag{2.59}$$

which express the local knot between the time-variation of the magnetic field and the induced electric field. This is one of the four Maxwell's equations.

The magnetic field B can be represented as rotor of another vector A called potential vector then replacing in (2.59)

$$\nabla \times E = -\frac{\partial}{\partial t}\nabla \times A = -\nabla \times \frac{\partial A}{\partial t} \Rightarrow E = -\frac{\partial A}{\partial t} \tag{2.60}$$

In general the E-field can be generated even by fixed charges then its equation in terms of the scalar electrostatic potential and potential vector is

$$E = -\frac{\partial A}{\partial t} - \nabla V \tag{2.61}$$

2. INSTRUMENTATION

2.1. INTRODUCTION

Sensors for electrostatic field [5] are employed in many applications either as stand-alone devices or as parts of more complex measurement systems (see section 11.3). Common applications concern surveying of fields generated by atmospheric phenomenon, transmission lines, particles detectors, mass spectrometers, scanning microscopes and electrophoresis systems [6], prevention of problems due to static charges either in processing and storage of inflammable materials and in the production of electronic devices. Automotive makes large use of such sensors for active and passive safety systems (such Air Bags), occupant sensing systems and touch controls [7]. Another interesting challenge pertain the areas of security and surveillance where they can be exploited to remotely detect weak biological fields produced by human bodies or animals.
Measurement of electrostatic fields requires the use of contactless systems to avoid surface discharging and potential alteration. Non-contacting instruments are commonly classified as electrostatic field meters (ESFM) and electrostatic voltmeters (ESVM).

2.2. ELECTROSTATIC FIELD METERS

Electrostatic field meters, also called static meters or static locators, measure the intensity of electrostatic field generated by a charged surface located some distance away using an high input impedance or chopper stabilized sensor that is referenced to ground. The sensor to surface distance must be known in order to obtain an accurate measurement; calibration of field meters must be performed before every measurement session [8], [5].
Electric field meters consist of two parts the probe or field sensing element and the detector which processes the signal from the probe and indicates the rms value of the electric field strength in units of V/m

using an analogue or digital display. They are of three types: free-body meters, ground reference meters and electro-optic meters [9].

2.2.1. FREE-BODY METERS

Free-body meters are based on the measure of the induced current between two isolated electrodes placed within the electric field. Thanks to their handiness due to reduced dimensions, battery-powered and electrically isolating from ground potential, they are suitable for fast evaluations. Geometries of commercial single-axis, free-body electric field meters are shown in Figure 2-3 [5].

Commercial field meters are usually rectangular in shape, and typical dimensions are on the order of 10 cm. A large dynamic range (1 V m^{-1} to 30 kV m^{-1}) is required to cover the various field sources (ac power lines, video display terminals, mass transportation systems, etc.) of interest.

A long, non conducting handle is normally attached perpendicular to the field meter axis for use in measurement surveys.

The charge Q on half of the field meter is proportional to the incident electric field E along the meter axis

$$Q = A\varepsilon_0 E \tag{2.62}$$

where A is a constant proportional to the surface area.

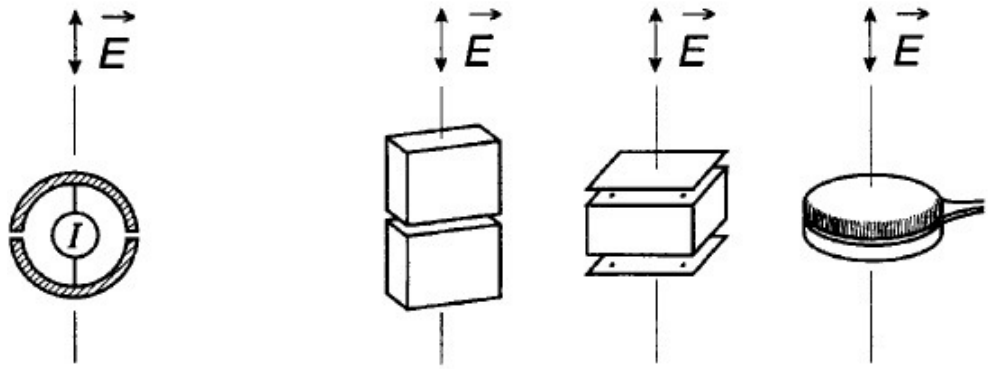

FIGURE 2-2 Geometries of commercial single-axis, free-body electric field meters.

For example for the spherical geometry $A = 3\pi a^2$, where a is the sphere's radius.

Since the current I between the two halves is equal to the time derivative of the charge, for time-harmonic fields it can be written

$$I = j\omega A\varepsilon_0 E \tag{2.63}$$

This allows E to be determined from the measured current.

For commercial field meters that are not spherical, the constant A needs to be determined by calibration. A known calibration field can be generated between a pair of parallel plates where the plates are sufficiently large compared to the separation to produce a uniform field with small edge effects [5]. This technique produces a well-characterized field with an uncertainty less than 0.5% [10]. However, the presence of harmonic frequencies can cause less accurate meter readings in field surveys.

For commercially available free-body meters, the detector is usually contained in or is an integral part of the probe. The probe and detector are supported in the electric field at the end of a horizontal insulating handle [10], [11]. The free-body meter is suitable for survey type measurements because it is portable, allows measurements above the ground plane, and does not require a ground reference potential.

There also exist free-body meters designed for remote display of the electric field strength. For this case, a portion of the signal processing circuit is contained in the probe and the remainder of the detector is in a separate enclosure with an analog or digital display. A fiber optic link connects the probe to the display unit [12], [13].

If the electric field strength has a sinusoidal time dependence, for example $E_0 \sin \omega t$ where ω is the angular frequency, the induced charge oscillates between the two halves and the current is given by

$$I = \frac{dQ}{dt} = A\omega\varepsilon_0 E_0 \cos \omega t \tag{2.64}$$

The constant A can be thought of as a field meter constant and is determined by calibration. The influence of the handle, representing a

leakage impedance, and the perturbation introduced by the observer are taken to be negligible in the above discussion.

If there are harmonics in the electric field, there will be an additional term on the right side of equation (2.64) for each harmonic. Because of the differentiation operation in equation (2.64), each of the additional terms will be weighted by the associated harmonic number. It is necessary for the detector to perform the inverse mathematical operation, namely integration, to recover the electric field waveform. This is accomplished by introducing a stage of integration. For example, an integrating amplifier or a passive integrating circuit combined with a voltmeter could be used as a detector. The frequency response of the probe-integrating detector combination should be made flat over the frequency range of interest. Filters should be used to exclude signals outside of the frequency range of interest.

2.2.2. GROUND REFERENCE METERS

Ground-referenced meters are normally used to measure the electric field strength at ground level or on grounded conducting surfaces and base their working principle on the measure of charge or current on a sensing electrode ground-referenced [5].

Two probe designs, shown in Figure 2-4, have been employed. One design makes use of a single flat conductor with an isolated central section that serves as the sensing surface. A second design consists of two parallel plates separated by a thin sheet of insulation, with the top plate acting as the sensing surface.

From Gauss' Law, the charge Q, induced on a sensing surface with area A, is

$$Q = \varepsilon_0 EA \tag{2.65}$$

where E is the average electric field strength across the sensing surface. Assuming that E varies sinusoidally with angular frequency ω

$$E = E_0 \sin \omega t \tag{2.66}$$

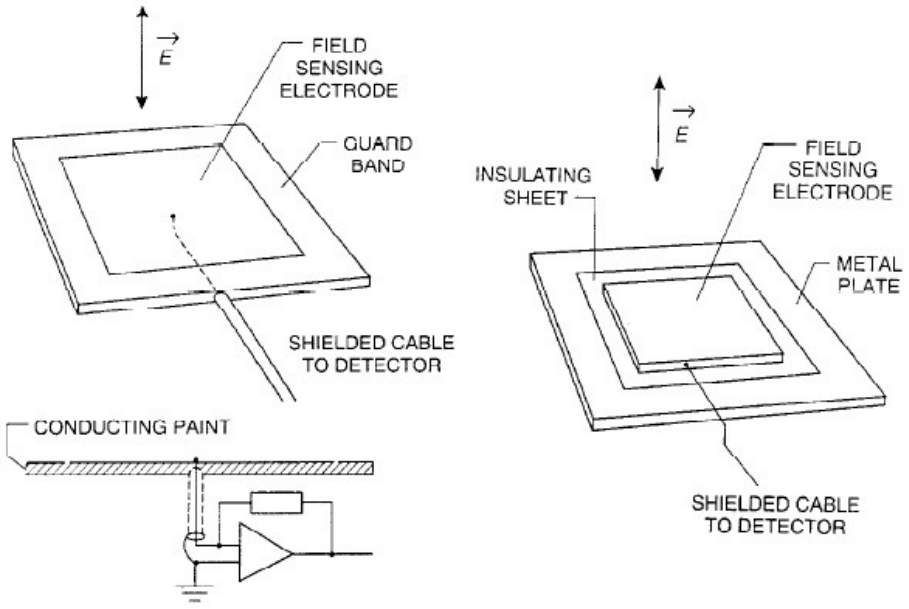

FIGURE 2-3 Two designs for flat probes used with ground-referenced electric field meters.

the resulting induced current is given by

$$I = \frac{dQ}{dt}\omega\varepsilon_0 E_0 A\cos\omega t \tag{2.67}$$

If there are harmonics in the electric field, there will be again an additional term on the right hand side of equation (2.67) for each harmonic and consequently because of the differentiation operation, each of the additional terms will be weighted by the associated harmonic number. To recover the electric field waveform, it is necessary to perform the inverse mathematical operation, namely integration. An integrating circuit/voltmeter combination that produces a flat frequency response over the frequency range of interest can serve as the detector. Filters also should be part of the detector circuit to exclude signals from outside of the frequency range of interest. Ground reference meters may be battery or mains operated.

Electric field meters with flat probes can be used to measure the electric field strength on flat electrically energized surfaces if the detector is

operated at the same potential as the energized surface. In such cases, viewing of the analog or digital display of the detector must be done remotely, either visually from a distance or using a fiber optic link.

2.2.3. ELECTRO-OPTIC METERS

Electro-optic field meters based on Pockels effect [5], [14], [15] are used in a similar fashion as free-body meters because they don't need ground-reference potential. A typical application is the investigation of radiofrequency electric field distributions. The probe is mechanically separated from remaining part of instrument and linked to him only by an optical fiber. The probe and detector are connected with optical fibers through which light from the detector is routed to and from the probe. Reduced dimensions of the probes (~2 cm) and insulation respect to surface charge distribution permit to perform measurement at reduced distances, thus improving the device resolution in the space domain, without the risk of electrical shots present with other field meters. However, Pockels effect probes have less sensitivity to electric fields (~5 kV/m and higher) compared to free-body meters (~1 V/m and higher) and are more expensive to fabricate [5].
Figure 2-5 shows a sketch of a Pockels effect probe and its constituent components. Light originating in the detector is sent to and from the probe via optical fibers. The electric field *E,* induces a birefringence in an appropriately oriented dielectric (Pockels) crystal that causes the intensity of the linearly polarized light to be modulated according to the relation [14]

$$\frac{I_t}{I_i} = \frac{[1 + \sin(E_\phi / F)]}{2} \tag{2.68}$$

where

I_t is the transmitted light

I_i is the incident light

E_Φ is the electric field in the crystal

F is equal to $\lambda / 2\pi n^3 c_e l$

λ is the wavelength of light

n is the index of refraction

l is the crystal thickness

c_e is the electro-optic coefficient of the crystal

For equation (2.68) to hold, it is assumed that the crystal has no intrinsic optical activity. Equation (2.68) shows that the amplitude of light modulation is a function of the electric field in the crystal that, in turn, is dependent on the external field E. Because the light transmission tracks the waveform of the electric field, a stage of integration is unnecessary in the detector to appropriately process signals due to harmonics that may be in the electric field. The Pockels crystal is sometimes coated with transparent electrodes to permit measurements of voltage using the Pockels effect. Electro-optic meters may be battery or mains operated.

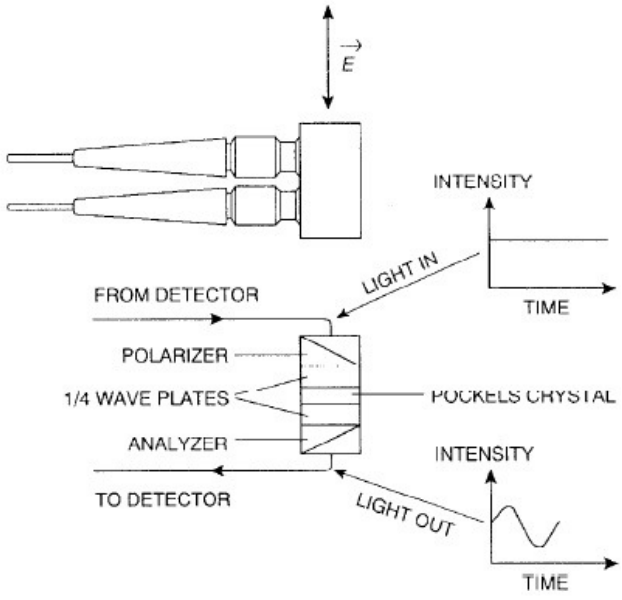

FIGURE 2-4 Probe for Pockels-effect electric field meter.

2.2.4. KELVIN PROBE

Another class of ESFM is the chopper–stabilized field meters whose main representative is the Kelvin probe [8], [16]
Most of instruments for non contacting measurements of electric field or surface potential are based on Kelvin probe. As an example the Kelvin Probe Force Microscopy (KPFM) also known as surface potential microscopy, a noncontact variant of Atomic Force Microscopy (AFM), that was invented in 1991 uses the working principle of the Kelvin probe [17].
Its working principle, proposed by Lord Kelvin in 1898, is based on the well known equation defining the capacitance of a capacitor C

$$C = \frac{Q}{\Delta V} \tag{2.69}$$

where Q is the gained electric charge while ΔV is the potential difference between the two electrodes. One of the most simple design of the Kelvin probe, shown in Figure 2-6, makes use of a parallel plates capacitor, whose capacity can be expressed as a first approximation as

$$C = \frac{\varepsilon_r \varepsilon_0 A}{D} \tag{2.70}$$

where A and D are the area of the sensing electrode and the distance of the sensing electrode from the surface, respectively.
In this system V_1 and V_2 correspond to the difference between the sensing electrode and surface potentials and the ground potential, respectively. If the charge Q^+ on the charged surface is constant, also the potential V_2 is constant; if the distance D is varied, e.g. moving away the sensing electrode, a corresponding variation of potential difference ΔV is observed. If also the potential V_1 is fixed by a suitable conditioning circuit, the variation of the coupling capacitance between the charged surface and the sensing electrode causes the removal or addition of charge dQ on the surface of the sensor. This consideration underlies the operation of the Kelvin probe. The amount of charge dQ extracted or introduced in a time dt is obtained by inverting and differentiating (2.69)

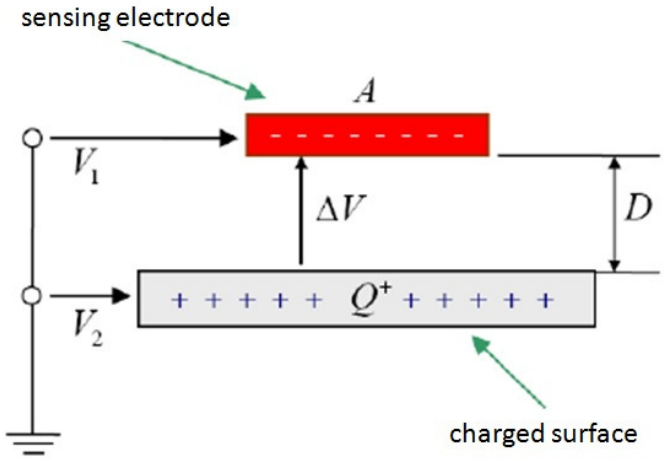

FIGURE 2-5 Working principle of the Kelvin probe.

$$\frac{dQ}{dt} = \frac{d(\Delta V \cdot C)}{dt} = \Delta V \cdot \varepsilon_0 \varepsilon_r A \cdot \frac{d}{dt}\left(\frac{1}{D(t)}\right) \tag{2.71}$$

Expressing the distance $D(t)$ as the sum of the nominal distance D_0 between the charged surface and the sensing electrode and the time variation $D_1(t)$

$$D(t) = D_0 + D_1(t) \tag{2.72}$$

it follows

$$\frac{dQ}{dt} = I(t) = -\Delta V \cdot \frac{\varepsilon_r \varepsilon_0 A}{[D_0 + D_1(t)]^2} \cdot \frac{dD(t)}{dt} \tag{2.73}$$

then it represents a current which flows through the electrode when the distance between it and the charged surface changes in time. This current is proportional to the speed of variation of $D(t)$.
Equation (2.73) can be inverted to evaluate the electric field generated by the charged surface

$$E = \frac{\Delta V}{D_0} = -\frac{I}{\varepsilon_r \varepsilon_0 A} \cdot \frac{[D_0 + D_1(t)]^2}{D_0}\left(\frac{dD(t)}{dt}\right)^{-1} \tag{2.74}$$

2.2.5. VIBRATING-REED METER

The vibrating-reed meter [18] developed by Gunn in 1932 is based on a Kelvin's probe vibrating in direction orthogonal to the charged plane as shown in Figure 2-7. The electrode moves according to a sinusoidal law with frequency ω then in this case equation (2.72) become

$$D(t) = D_0 + D_1 \sin \omega t \tag{2.75}$$

Replacing (2.75) in (2.70) it follows

$$C = \frac{\varepsilon_r \varepsilon_0 A}{D_0 + D_1 \sin \omega t} \tag{2.76}$$

then the induced current is

$$I = \Delta V \cdot \frac{dC}{dt} = -\Delta V \cdot \varepsilon_r \varepsilon_0 A \cdot \frac{\omega \cdot D_1 \cos \omega t}{\left(D_0 + D_1 \sin \omega t\right)^2} \tag{2.77}$$

By inverting (2.77) it can be evaluated the electric field produced by the charged surface

$$E = \frac{\Delta V}{D_0} = -\frac{I(t)}{\varepsilon_r \varepsilon_0 \omega A} \cdot \frac{\left(D_0 + D_1 \sin \omega t\right)^2}{D_0 D_1 \cos \omega t} \tag{2.78}$$

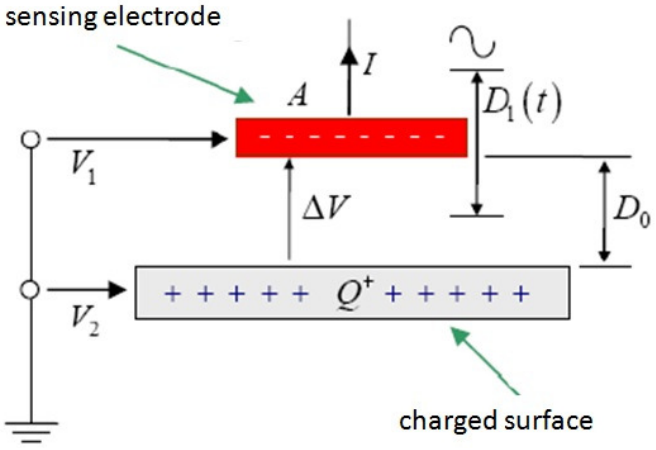

FIGURE 2-6 Vibrating-reed meter.

Riehl and coauthors in [6] have described the development of a high resolution MEMS-based vibrating reed-meter-like electrometer having a charge resolution of 4.5 aC rms (28 electrons) in a 0.3 Hz bandwidth.

2.2.6. VIBRATING WIRE METER

The vibrating wire meter developed by Struminsky is constituted by three parallel metallic bars in which that in central position is grounded and free to oscillate in the direction of the unknown electric field E_0, while the other two are fixed [19] . A schematic of the device is shown in Figure 2-8.

If the central ferromagnetic bar oscillates with frequency ω (typically 300 Hz) it produces a modulation of the electric field inducing a current on the lateral non-magnetic bars which will be converted in a tension by a current-to-voltage converter

$$V_{out} = -n\varepsilon_0\varepsilon_r E_0 \sin(\omega t + \psi) \tag{2.79}$$

where

n is a sperimentally evaluated constant

ψ is phase constant whose value is $\psi = \pi/2 - \arctan(\omega R_f C_f)$

ε_r is the relative electric permittivity of the environment

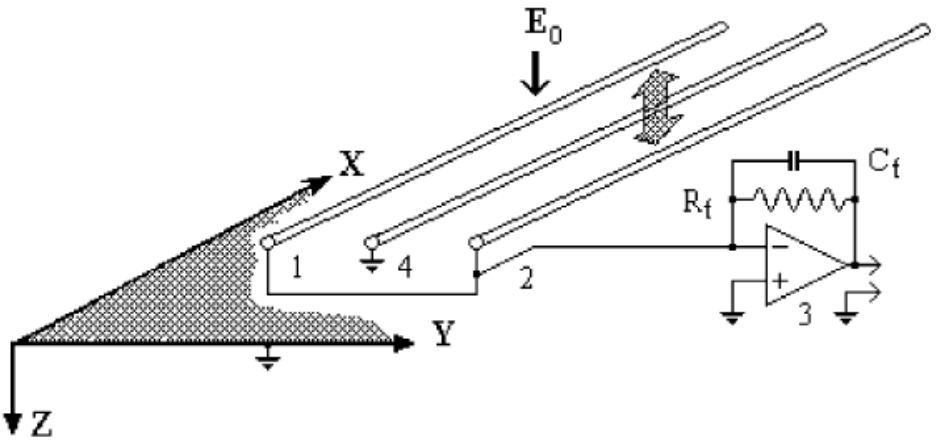

FIGURE 2-7 Vibrating wire meter with conditioning circuit.

TABLE 2-1 Main parameters of vibrating-wire field meter

Sensitivity (noise level)	0.2 V/m
Dynamic range	60 dB
Transformation frequency	300 – 500 Hz (adjustable)
Output voltage range	+5 to -5 V
Power supply consumption	~ 0.6 W
Weight	~ 0.9 kg
Dimensions	200 x 60 x 25 mm

The main operational parameters of the described instrument are given in Table 2-1.

The sensor operating in an outdoor atmosphere is under the influence of a wide range of environmental factors, e.g., varying temperature and humidity of the medium, wind, and precipitation such as rain or snow. In this case it is necessary to incorporate additional measures for stabilization of its gain and lowering of longtime zero drift.

2.2.7. LATERALLY VIBRATING KELVIN PROBE

In the laterally vibrating Kelvin probe the sensing electrode oscillates in direction parallel to the surface being measured at a specified distance, as shown in Figure 2-9 [16]. This technique is called the induction or scanning mode [20].

If the distance D is maintained constant while the electrode moves laterally along the charged surface, the capacitance C of the system is theoretically constant; however for non well-conducting surfaces that is in presence of local variations of charge the potential difference ΔV varies. As a consequence a current is produced given by

$$I(t) = \frac{d}{dt}\left(\Delta V(t) \cdot C\right) = C \cdot \frac{d(\Delta V(t))}{dt} \tag{2.80}$$

Inverting and integrating (2.80) the electric field can be evaluated as it follows

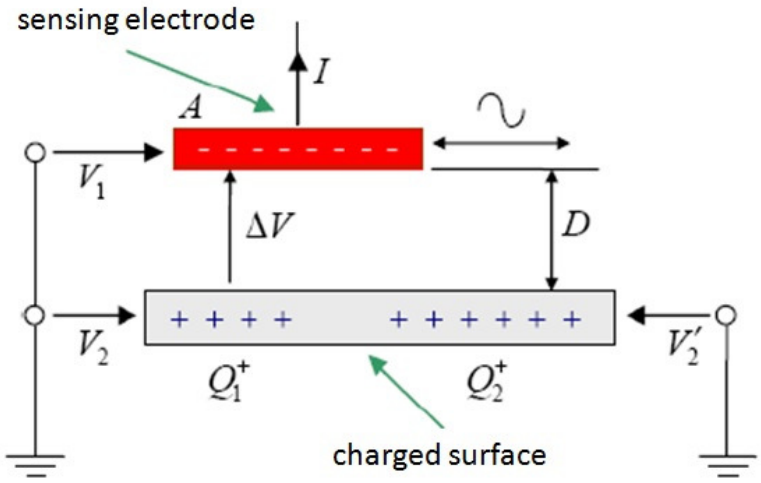

FIGURE 2-8 Laterally vibrating Kelvin probe.

$$E = \frac{\Delta V(t)}{D} = \frac{1}{C \cdot D} \cdot \int I(t)dt \tag{2.81}$$

From (2.80) it can be observed that greater is the speed of vibration greater is the detected current. The limit of this "scanning" technique has to be researched in the compromise between resolution and sensitivity depending both on the dimensions of the sensor: bigger sensors give lower resolution measurements; on the other hand, being the amplitude of the current $I(t)$ proportional to the capacitance smaller areas give lower sensitivity.

2.2.8. FIELD MILL (GENERATING VOLTMETER)

All of the above devices sense the electrostatic field at their sensing electrodes and use mechanical modulators to convert a DC field into an AC field [21] inducing a sinusoidal displacement current in the sensing electrode, whose magnitude is proportional to the electrostatic field intensity. Such an analogue principle is the base of the most popular measurement instruments for electrostatic fields: the field mills [22]. The main difference is that the electrode vibrates on a surface partly

covered by a reference electrode having a known constant potential. The measured current will be given by two contributions: the possible non uniform distribution of charge and the variation of capacitance.
In the technical literature, two types of field mill are described: the shutter type and the cylindrical type [22].
The first one, developed in 1950, is the most common used and shows high sensitivity. It has a sensing electrode that is periodically exposed and shielded from the electric field by a grounded rotating shutter with a typical frequency of 20-50 turns per second. Shutter-type field mills are usually operated with the shutter nearly flush with the ground plane.
The induced charge at any instant, q_s as well as the induced current i_s between ground and the sensing electrode as the sensing electrode is alternately exposed and shielded, are proportional to the electric-field strength E

$$q_s = \varepsilon_0 E\, a(t) \tag{2.82}$$

where $a(t)$ is the exposed area of the sensing electrode at time t.
The induced current is found by taking the derivative of equation (2.82)

$$i_s(t) = \frac{dq_s(t)}{dt} = \varepsilon_0 E \frac{da(t)}{dt} \tag{2.83}$$

Thus, the field strength can be determined by measurement of the induced charge, current, or voltage across an impedance that is located between the sensing electrode and ground.
A simplified schematic view of a shutter-type field mill is shown in Figure 2-10. Two commercial devices are also shown in the same figure. The grounded rotating shutter periodically shields the sensing electrode, as shown in Figure 2-11, which leads to a time-varying current between ground and the sensing electrode [23].
If the induced-current signal is rectified by a phase-sensitive detector operating with a suitable phase angle relation to the motion of the shutter, the dc signal output will indicate the polarity and magnitude of the electric-field strength [24].

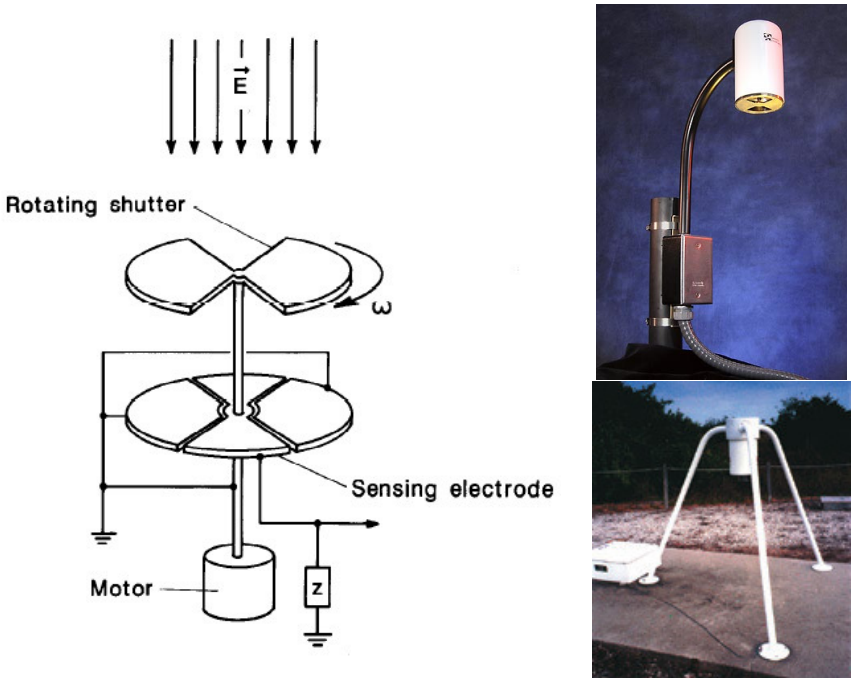

FIGURE 2-9 Simplified Schematic View of a Shutter-Type Electric Field Mill and two commercial devices.

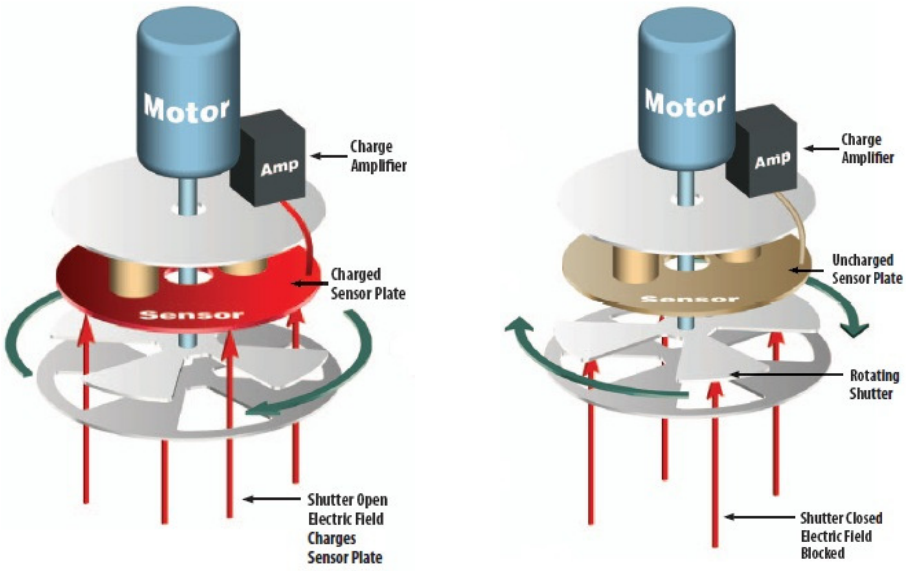

FIGURE 2-10 Field mill operation [23].

Because of the presence of space charge in the vicinity of dc power lines, it is possible to have, in addition to the induced current, conduction current (of ions) to the sensing electrodes of the field meter.
This additional current, which is chopped by the rotating shutter, represents an error signal and shall be corrected in the instrumentation. One approach is to use phase-sensitive signal processing that discriminates against the conduction current, which is in quadrature with the induced-current signal [24].
While shutter-type field mills are normally operated in the ground plane in order to measure the field at ground level, measurements of the field at ground level can also be made with a field mill that is mounted on a stand, provided the measurements are corrected for the associated field enhancement through some calibration procedure. It should be noted that the geometry that exists during the calibration process shall be maintained during the measurements. For example, if grass or weeds are allowed to grow near the stand, the effective ground plane could rise. Similarly, the ground plane would be affected by the accumulation of snow on the ground [22].

Alterations of measurement can be due to the size of surface being measured in relation to the sensing area of the device, the relation of the charged surface to ground and the presence of other objects in proximity to the surface [25]. As a consequence, these meters must be calibrated from time to time with relation to working status placing it to a fixed distance from a large flat plate in free space that is charged to a specific voltage. During the measurements, the observer should be well removed from the measurement location to avoid perturbing the electric field. More details about calibration of instrumentation and sources of measurement errors can be found in [5].
If the surface presents voltage gradients the meters will indicate the average surface potential. Electrostatic field meters don't represent the best choice when high resolution measurements are requested. Nevertheless they are versatile, can measure high voltages at large distances and are cheap.
Some signal processing occurs in the housing that contains the sensing electrode and shutter. The remainder of the signal-processing circuit

and field-strength display are contained in a shielded enclosure that is connected to the sensing electrode housing with a shielded cable.

Because the electric field in the vicinity of a dc power line is not uniform, it may be of interest to measure the electric field strength at points above the ground plane. This can be done with the second type of field mill, the cylindrical field mill [22]. Typically, the charges are induced by the electric field on two exposed half-cylinder sensing electrodes. The induced charges on the sensing electrodes are varied periodically by rotating the sensing electrodes about the cylinder axis at a constant angular frequency, as shown schematically in Figure 2-12. Expressions for the induced charge q_c and current i_c between the half-cylinders for a cylinder of length L and radius r_0, ignoring end effects, are [26]

$$q_c = 4\varepsilon_0 r_0 LE \sin \omega t \tag{2.84}$$

and

$$i_c = 4\varepsilon_0 r_0 LE\omega \cos \omega t \tag{2.85}$$

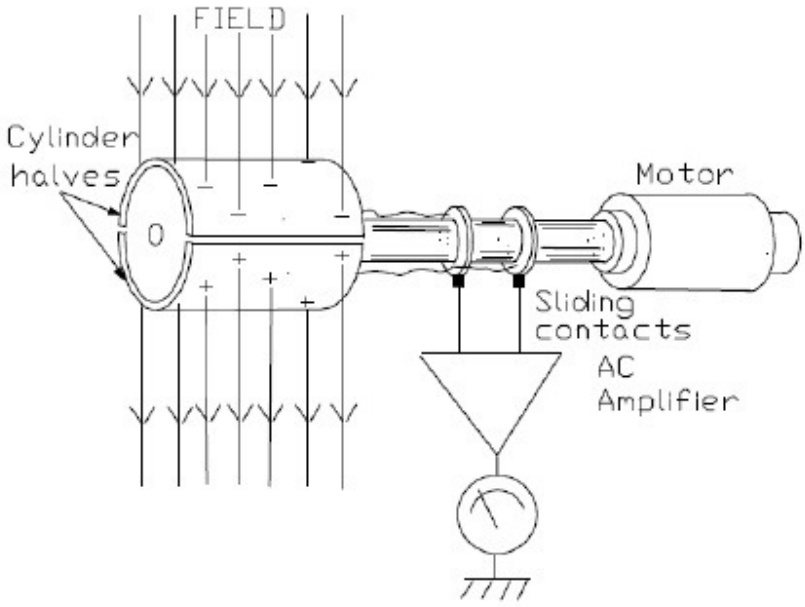

FIGURE 2-11 Schematic View of a Cylindrical Field Mill.

Cylindrical field mills that operate at near space potential [13], [27], [28], and at ground potential [29] have been developed for measurements above the ground plane near dc power lines.
For both cases, the field at the surface of the cylinder will be a superposition of two components, one due to the field from the dc power line (distorted by the cylindrical probe) and the other due to a constant, symmetrically distributed charge on the cylinder. Because no electrical signal is generated by the symmetrically distributed self-charge as the cylinder rotates [28], the signal that is produced is due to the time-varying induced charge or current approximately described by (2.84) and (2.85) and, as for the case of the shutter-type field mill, a time-varying ion current due to the space charge in the field. In order to determine the electric field strength with both currents present, ground-referenced cylindrical field mills require two sets of rotating cylinders with different frequencies of rotation [29]. In an electrically isolated cylindrical field mill the self-charge uniformly distributed on the cylinder is of opposite polarity and results from a charging process due to ions in the field impinging on the cylinder. The cylinder becomes fully charged in a negligible time and prevents the further flow of ions to the sensing electrodes. Thus, the need for a second set of sensing electrodes rotating at a different frequency, as required for the ground-referenced cylindrical field mill, is eliminated.

The field mill working principle underpins the devices described either in [6] by Riehl and co-authors and in [30] by Chao and coworkers. In both works novel MEMS-based electrostatic field meter having a resolution of 630 V/m and 1kV/m, respectively, are described.

2.2.9. SIGNAL CONDITIONING AND PERFORMANCE LIMITS

A schematization of the typical conditioning circuit [21] for signals coming from the Kelvin probe is shown in Figure 2-13.
The AC signal induced on the sensor by the movement of the sensing electrode is sent to a preamplifier typically placed within the probe. The signal is then processed by a phase demodulator together with the signal coming from the oscillator which drives the electromechanical

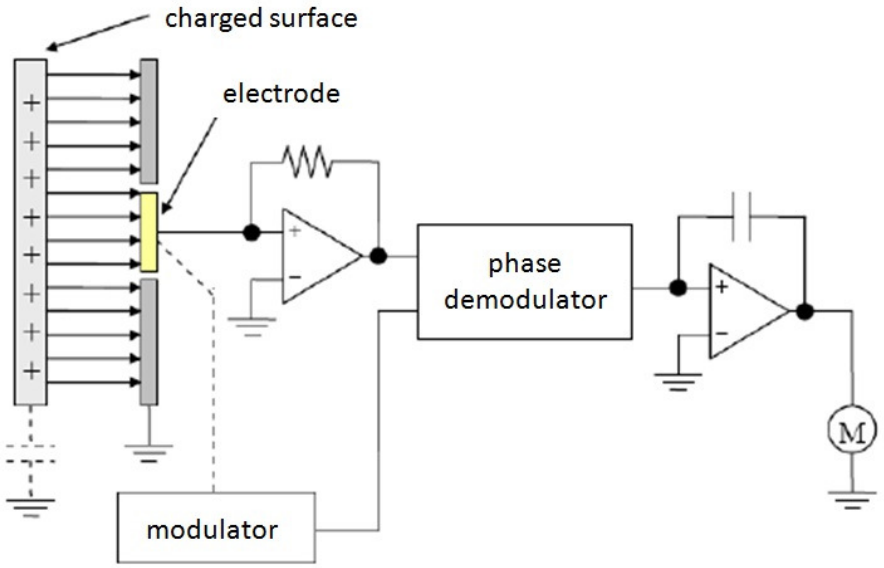

FIGURE 2-12 Schematization of the conditioning circuit for Kelvin probe.

modulator. The output signal is a DC voltage whose sign and amplitude depend on the potential difference between the inputs and then on the sign and the electric field strength. The DC voltage is finally supplied to an integrator working as a charge amplifier whose output voltage is proportional to the electric field.

Performances of the Kelvin probe and of instruments based on it, in terms of sensitivity and accuracy, depend on a correct design and employment. Design must take in account possible sources of noise, parasitic capacitances and ionizing radiations. The correct employment depend on careful calibration, an optimal distance from the quantity to measure and an optimized geometry of the system. In particular the following criticalities can be identified.

Presence of ions

Ions can produce a conduction current which adds to the current induced by the modulations. To the purpose to separate the two currents suitable signal conditioning techniques must be employed [22].

Noise

The Kelvin probe is much sensible to electromagnetic noise (electric fields and induced charges) and to mechanical noise (vibrations). In particular in the field mills apart the vibrations due to the rotating axes, the electrical micro-discharges due to the brushes contacting the sensing electrode are present. The problem can be minimized with a suitable electric shield and employing suitable motors (ball bearing, brushless DC motors).

Charge gathering

The dust on the sensor can produce a charge gathering which generates an offset on the output voltage. To remedy this drawback the probe and all the parts directly exposed to the electric field must be cleaned

Distance from surface

The quality of the measure depend on the precision of the measurement of the distance from the charged surface. From equation (2.77) it is evident that the sensitivity is lower as the distance D is greater; on the other hand an increment of the D makes worse the resolution, as shown in Figure 2-14, due to both the angle of vision of the probe and to the border effect. To limit the border effect, generally guard ring around the sensing electrode are employed as shown in Figure 1-15.

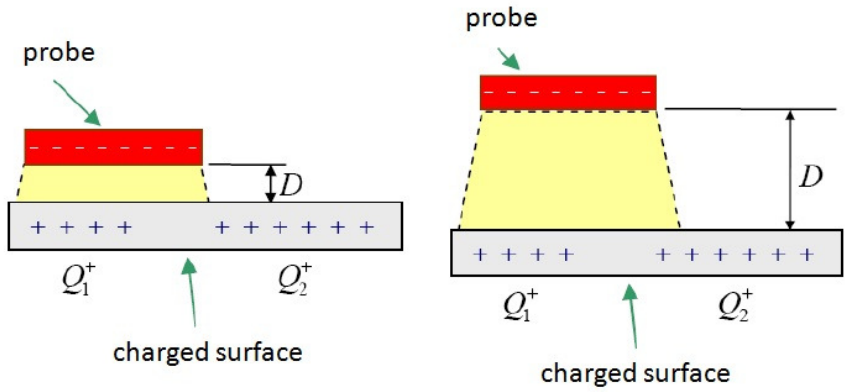

FIGURE 2-13 Dependence of the resolution on the distance of the sensing electrode from the charged surface.

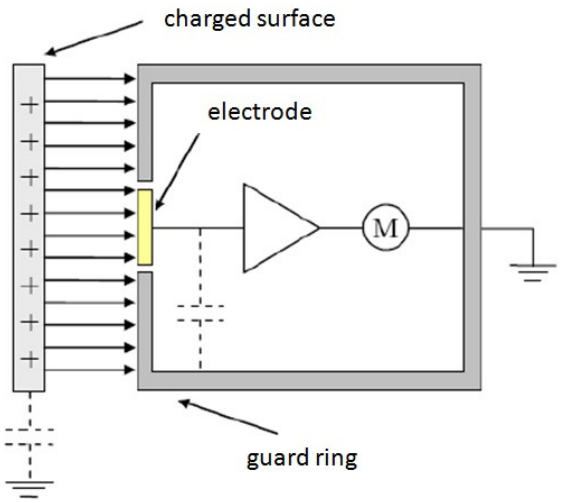

FIGURE 2-14 Shielding of the sensing electrode with guard ring.

In [21] Pritchard has investigated the capabilities and limitations of both electrostatic field meters and electrostatic voltmeters (discussed in section 11.2) for making measurements on small objects such as GMR recording heads. Without giving details on the experiments (see [21]) he concluded that each type of electrostatic field meter and electrostatic voltmeter has a set of capabilities and limitations that determines the missions it is best suited to perform. While electrostatic field meters are well suited for auditing large surface areas for charge accumulations, electrostatic voltmeters, when used properly, are better suited for making measurements of small objects.

Parasitic capacitances

The Kelvin probe is affected even by the capacitive coupling with all the objects in the surrounding environment connected to the ground, such as mechanical parts, wires, operators etc.
Even all these parasitic capacitances are modulated by the vibration of the probe and give a contribution to the measured current. To avoid this effects it is necessary to remove these objects from the environment or to shield the probe or, alternatively, to correct them during the calibration phase [5], [31].

2.2.10. RADIOACTIVE FIELD METERS

Radioactive field meters are based on the use of radioactive components which ionize aria closeness to the probe. If an electric field exists, it produces a proportional conduction current detectable by proper conditioning circuits as that shown in Figure 2-13. They are very simple in spite of the use of radioactive substances; moreover a long term deterioration of performance, due to accumulation of spurious elements on it, is experienced.

2.2.11. VIBRATING PLATE ELECTRIC FIELD METERS

A simplified schematic view of a probe with a vibrating plate sensing electrode is shown in Figure 2-16. Charges induced on the plate below the aperture by the electric field are modulated by the vibrational action of the mechanical driver [32], [33], [34], [35]. For the configuration shown in Figure 1-16, the field meter responds to the negative charges induced on the vibrating plate by generating a negative feedback voltage V_{fb} to the faceplate to null the signal from the vibrating plate V_s; the electric field strength is proportional to the feedback voltage [35]. As in the case of the shutter-type field mill, the vibrating plate probe is mounted flush with the ground plane during use, and a portion of the signal-processing circuit and field strength display are located remotely in a shielded box. The observer should be sufficiently removed from the measurement location to avoid perturbing the electric field.

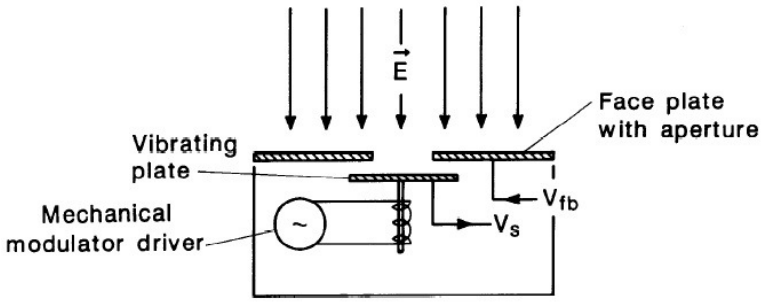

FIGURE 2-15 Schematic View of Vibrating Plate Electric-Field Meter Probe.

2.2.12. DESIRABLE FIELD METER CHARACTERISTICS

Electrical characteristics

Power supply. The instrument should employ a self-contained power supply that is isolated from external electric fields. If batteries are used, provision should be made for indicating their condition. Survey type and personal exposure recording instruments should be capable of at least 8h operation within its rated accuracy before replacement or recharging of the batteries becomes necessary.

Precision and accuracy. The instrument should be provided with calibration data or instrument specifications that permits the user to assess the maximum uncertainty in determining field levels when using the instrument in fields containing different frequencies. This information should also include the sensitivity of the instrument to frequencies beyond the intended useful range.

Physical characteristics

Portability. The instrument should be portable to permit, where appropriate, convenient operation under restrictive conditions, e.g., climbing a tower with a survey meter.

Weight. The weight should be kept as low as is practical in keeping with good engineering practice.

Volume. The volume should be as small as is practical and convenient for, when appropriate, hand-held operation.

Dependence on temperature and humidity. The specified accuracy of the instrument should include the effects of temperature and humidity, and the operating ranges for these parameters should be indicated.

Durability. The indicating meter and other system components should be rugged enough to withstand vibration and shock resulting from transport. A carrying case is desirable.

Readability. The meter dial markings or digital displays of magnetic field meters should be large enough to be easily read at arm's length. The meter dial markings or digital display of free-body electric field

meters should be large enough to be read at greater distances to avoid perturbations of the electric field due to proximity effects of the observer. If more than one range of sensitivity is provided, the full scale value of the selected range should be indicated and the units should be readily interpretable. For auto-ranging instrumentation, the dynamic range may be indicated elsewhere, e.g., in the user manual. The instrumentation should provide a clear indication of the units being displayed. To comply with this standard, instrumentation marketed prior to the issue of this standard, that do not indicate the units, should be provided with an appropriate label indicating the units. This may be accomplished by the user applying a label to the body of the field meter. Alternatively, a label provided by the manufacturer to the user, may be applied by the user.

Ease of adjustment. The instrument should have a minimum number of controls. They should be clearly labeled as to their functions.

Location and orientation of coil probes. The locations and orientations of coil probes that are contained within the housings of magnetic field meters should be clearly indicated on the instrument or in the instruction manual.

2.3. ELECTROSTATIC VOLT METERS

The second class of instruments is that of electrostatic voltmeters which measure the actual potential (voltage) at the surface of the object under test using a non contacting sensor, without introducing a loading effect. Generally they are based on an oscillating Kelvin probe to obtain a current in the sensing electrode which is not the quantity to measure rather to annul by a feedback. So, measuring of potential becomes very careful and with a good approximation independent from probe-to-surface distance. Measurement accuracy is typically 0.1% regardless of probe-to-surface spacing (spacing is usually in the range of 2.5 mm) with a target resolution 2.5 mm or smaller. Electrostatic voltmeters typically can measure over the range from millivolts to several thousand volts. Depending on the magnitude of voltage to be measured, two types

of voltmeters can be employed: the DC feedback electrostatic voltmeters and the AC feedback electrostatic voltmeters.

2.3.1. DC FEEDBACK ELECTROSTATIC VOLTMETER

The DC-feedback electrostatic voltmeter uses a DC voltage to null the electric field between the charged surface and the probe. This method minimizes capacitive loading of the charged surface and more accurately reports the electrical potential of the tested object, which can be as high as 10 kV or more [8]. Consequently, it is necessary to use high voltage circuitry and high speed amplifier circuitry capable of following sudden changes in measured voltages. All these requirements influence the cost of the device.

The working principle is schematized in Figure 2-17 where a vibrating reed meter is considered as sensor.

If a potential difference exist between the guard ring of the sensor and the charged surface an AC current is induced on the sensing electrode by the capacitance modulation. As already seen for the field meters (see Figure 2-13) this current is conditioned up to the output of the integrator. Then the signal is passed to an high voltage (HV) amplifier whose output voltage will be the reference potential of the probe which will tends to follow the potential of the charged surface.

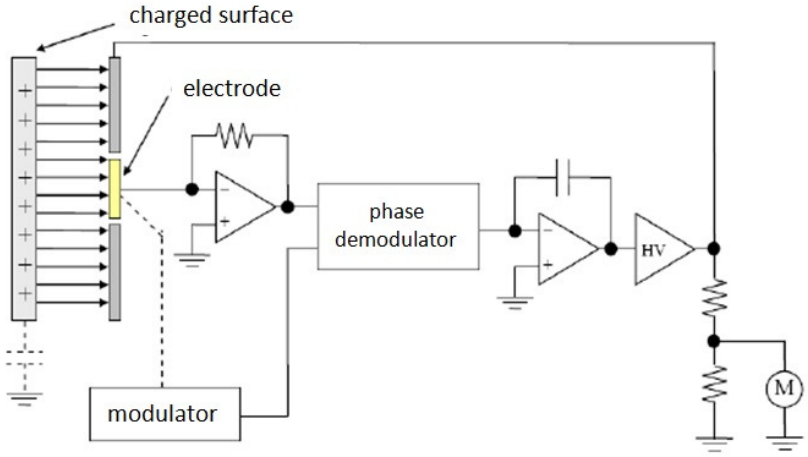

FIGURE 2-16 Schematization of a DC-feedback electrostatic voltmeter.

When the two potential became equals, that is when the output voltage of the high voltage amplifier became equals to the unknown potential, the measurement process is in the regime state. From equation (2.77) it follows that the induced current is null and the output of the integrator is constant. The voltage can then be acquired from the output of the HV amplifier by a voltage divider and sent to an indicator.

2.3.2 AC FEEDBACK ELECTROSTATIC VOLTMER

AC feedback electrostatic voltmeters [8] combine the low cost of field meters with the accuracy of DC feedback voltmeters avoiding high voltage electronics. Moreover they offer spacing-independent measures with better accuracy than field meters.
A schematization of the voltmeter is shown in Figure 2-18. Their working principle is based on the feedback of a low AC voltage to null the total current I with a current I_f equals but opposite to the current I_m due to the capacitance modulation

$$I = \frac{dQ}{dt} = \frac{d(C \cdot \Delta V)}{dt} = \underbrace{C \cdot \frac{d(\Delta V)}{dt}}_{I_f} + \underbrace{\Delta V \cdot \frac{dC}{dt}}_{I_m} = 0 \tag{2.86}$$

From equations (2.77) and (2.86) it follows that

$$I_f = \Delta V \cdot \varepsilon_r \varepsilon_0 A \cdot \frac{D_1 \omega \cos(\omega t)}{\left[D_0 + D_1 \sin(\omega t)\right]^2} \tag{2.87}$$

and inverting the last equation it is possible to evaluate the surface potential $V_s = \Delta V$

$$V_s = \frac{I_f}{\varepsilon_r \varepsilon_0 A} \cdot \frac{\left[D_0 + D_1 \sin(\omega t)\right]^2}{D_1 \omega \cos(\omega t)} \tag{2.88}$$

The AC feedback ESVM is a middle way between a field meter and a voltmeter: from the first device it has the ground potential reference and the risk of discharge for small distances; from the second class of devices it has the measured quantity (the surface potential) and the accuracy which is distance independent as shown in Figure 2-19.

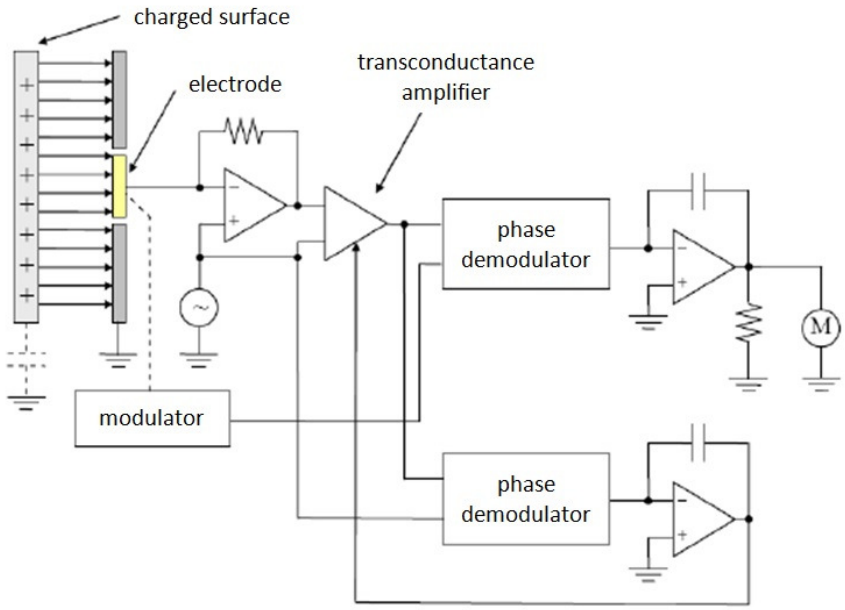

FIGURE 2-17 Schematization of the AC feedback electrostatic voltmeter.

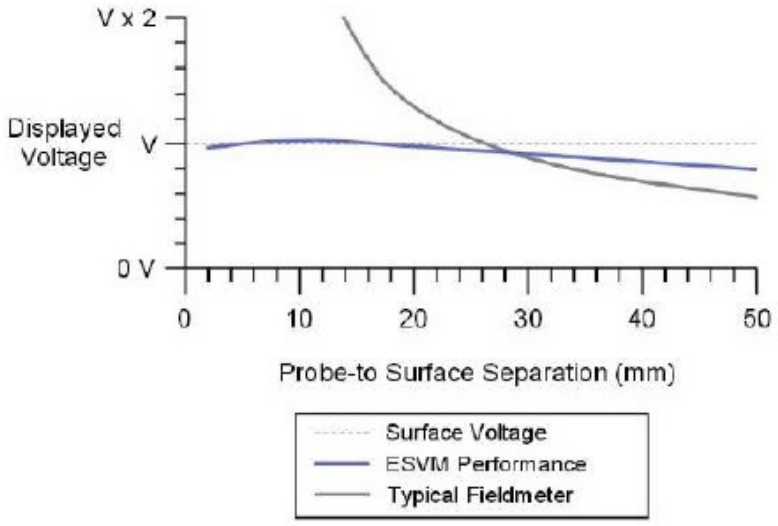

FIGURE 2-18 Measured voltage vs distance for field meter and AC feedback ESVM.

The distance D_0, for which AC-feedback voltmeter achieves its maximum accuracy, is limited by several factors. First factor is the D_0/D_1 ratio which determines the minimum plate-to-sensor spacing. Another element limiting that minimum is the voltage difference between the plate and the sensor. Notice that, unlike in the DC-feedback ESVM, AC-feedback technique does not bring the potential on the sensor to that of the surface under test.

There is a possibility of an electric discharge between the sensor and the plate, which can lead to damage of the voltmeter. There is also a limit regarding the maximum distance D_0. It depends on the size of the sensor, if an influence of environmental conditions can be considered negligible. If the sensor is too far from the tested surface, it becomes capacitively coupled to the surrounding, i.e. test equipment, furniture, etc. An additional constraint for AC-feedback ESVMs pertains to the type of surfaces that can be examined with accuracy specified by the manufacturer. If capacitance between the tested object and the earth ground is comparable to or less than the probe-to-ground capacitance, the AC-feedback voltmeter readings become inaccurate [36].

The AC signal generated by the AC-feedback is being induced on the surface due to the capacitive coupling between the probe and the surface under test. The AC component present on the tested object creates an error offset voltage.

2.4. E-FIELD SENSORS APPLICATIONS

Sensors for electric field monitoring are employed in many applications either as stand-alone devices or as parts of more complex measurement systems. Looking through the scientific literature or surfing the web a lot of disparate applications can be discovered and many others are continuously proposed mainly because permit to have reliable contactless and not invasive systems in a world where it has been found to be much to sense. In the following a classification of applications is presented. The list presented here has no pretences of being complete and exhaustive, rather it aims to give an idea of the many and varied

applications. Some of the reported applications may be considered to belong to more classes.

E-field emission monitoring

Applications pertaining this class deals with the monitoring of E-field emissions in both outdoor and indoor environments and how they might relate to human exposure.
Examples of these applications are:

- the measurement of the electric-field strength, ion-current density, conductivity, monopolar space-charge density, and net space-charge density in the vicinity of high voltage (HV) power lines, in converter substations, and in apparatus designed to simulate the HV power-line environment [22], [25].
- the measurement of the root-mean-square values of electric fields in residences, the work place, and transportation systems [5].
- the measurement of electric fields produced by video display terminals (VDT), appliances, and other electrical equipment [9].

Industrial applications

An extensive employment of e-field sensors can be recognized in industrial applications:

- in the semiconductor fabrication and assembly e-field sensors are employed in most ESD and EOS sensitive electronic manufacturing processes to evaluate small charges on small surface areas which may damage the product being manufactured or bring about malfunction in the manufacturing equipments. E-field sensors can be used to control an air ionization system to keep the manufacturing process in a safe condition, or to provide danger alarm [30].
- point of sales terminals [37].
- refrigeration frost sensors [38].

- monitoring the changing state of a polymer in a composite (or in an adhesive joint or as a coating) during fabrication and aging during use in the field [39].
- to monitor cure in production ovens and autoclaves on the plant floor as well as outside, for example, coatings on the surface of a ship in dry dock [39].
- touch and proximity sensors for industrial robots [40].
- investigation of surface and sub-surface structures (variations in the composition and density of material structures and the presence of an internal mass in a building structure) [41].
- tomography applications to investigate the moisture content in food products, pharmaceutical products, pape pulp [42].
- electrophotography [43].
- measurements on GMR recording heads [21].
- nondestructive evaluation (NDE) technique that measures geometry and structural variations in nonmetallic engineered materials [44].
- quantitative assessment of the condition of thermal barrier coatings (TBCs) [45].
- spill over flow sensing measurement [38].
- liquid level sensing [38].
- detecting the ionization level of a gas mixture [46].

Security and surveillance

An interesting challenge pertain the areas of security and surveillance in military applications, automotive and industry:

- detection and localization [47], [48].
- garage door safety sensing [38].

- workers worn e-field sensors [49].
- authentication and access control systems [50].
- vehicles classification [51].
- arming apparatus for an explosive projectile [52].
- automotive safety sensing: capacitive sensing for presence in auto and seat occupancy classification [53], [38].
- keyless entry systems and tire pressure [54]
- industrial Control and Safety Systems Security [38].
- detecting the strength of an electrostatic field in the vicinity of an aircraft [55]

Scientific applications

Many scientific apparatus make use of electric field sensor because their reliability and the possibility to make experiments without contacting the system under investigation:

- mass spectrometers [56].
- scanning-tunneling microscopes [6].
- electrophoresis systems [6].
- weather phenomena investigations: atmospheric e-field, thunderstorm electricity and lighting [57].
- ambient e-fields in proximity of the surface of a satellite and high-altitude rocket [19], [30], [58].
- long-term field monitoring at continental stations [19].
- field measuring on board a scientific ship in oceanographic expedictions [19].
- estimation of direction of arrivals waves in a Borehole radar [59].
- hyperthermia applications [15].

- e-field in sea water [60], [61].
- downhole telemetry [62].
- geophysical exploration [63].

Biological and medical applications

E-field sensor are largely employed in medical applications and biological analysis and now increasingly in health care monitoring:

- nuclear magnetic resonance (NMR) [64].
- lab-on-chip Bio-cell detection micro array [65].
- tomography [42].
- ECG/EEG signal sensing [66], [67], [68]
- health care patient monitors [37]

Multimedia, entertainment, interfaces and others

In this class have been collected all the applications related to multimedia, entertainment and alternative human-machine interfaces and other areas.

- musical applications [69]
- e-field sensing for detecting static thumb position [70]
- enabling third dimension in PC peripherals [71], [72]
- human-computer and human-machine interface [73]
- virtual reality [73]
- multimedia devices [74]
- appliance control panels and touch sensors [38]
- linear and rotational sliders [38]
- touch screens [38]

- detecting pulses due to electrostatic discharges from furniture or human beings [75]

2.5. THE PROPOSED STRATEGY FOR E-FIELD EVALUATION

All afore mentioned devices, are based on classical linear relationships governing electrostatic phenomena.
In this thesis an alternative and unconventional methodology exploiting the potentiality of sensing solutions based on nonlinear coupled detectors is addressed and discussed in the following chapters.
The possibility to exploit nonlinear ferroelectric devices to sense static and quasi-static DC electric field is discussed along with real evidences of the methodology effectiveness [76], [40]-[44].

CHAPTER 3

FERROELECTRICS, THEORY AND APPLICATIONS

You don't need as much the desire to believe as rather to discover, which is exactly the opposite.
- Bertrand W. A. Russell

1. HISTORICAL INTRODUCTION

Ferroelectrics are a class of high dielectric permittivity materials. They are polar materials characterized by a transition to a paraelectric, nonpolar phase at a temperature at which their dielectric permittivity presents a maximum. Ferroelectrics are also a group of materials whose crystalline structure possesses a crystallographic axis (polar axis) in the direction of which there is a spontaneous polarization in the polar phase, arising from a displacement of positive and negative centers of charge of the ions in the structure, whose sign can be reversed by a sufficiently high electric field.

Ferroelectric, from the German "ferroelecktrisch," was a term coined in 1912 by Erwin Schrodinger in his "Habilitations-Schrift" submitted at the University of Vienna [77], who, as an extension of Peter Debye's model for gases and liquids [78], speculated that in solids below a certain temperature, analogous to the Curie temperature of the ferromagnetic materials, a permanent polarization ought to be expected in the absence of an electric field. However, no such phenomenon had been observed so far [79].

1.1. ROCHELLE SALT

Ferroelectricity, which at the time was called Seignette-electricity, was reported for the first time by Joseph Valasek (1897-1993), who worked at the University of Minnesota in Minneapolis, in [80] at the meeting of the American Physical Society in Washington, in 1920. Rochelle salt is a water-soluble compound that was prepared in 1665 by Elie Seignette (1632-1689), a pharmacist at La Rochelle (France), for medical purposes.

He called it sel polychreste, salt of various utilities, and kept secret the way in which he produced it [81]. Sixty-five years after it was first prepared, it was identified by Simon Boulduc, a Parisian chemist, as "some tartrate of soda" [82]. It is the sodium potassium salt of tartaric acid with four molecules of water of crystallization. It is likely that Elie Seignette started from crème of tartrate (potassium hydrogen tartrate) he obtained from wines – so famous and abound in the Bordeaux region – and soda which makes the tartrate soluble in water. The "sel polychreste" – or Rochelle salt as we know it today - conquered the market in France, especially in Paris and it was in widespread use for more than two centuries as a mild drug. The chemical formula is $NaKC_4H_4O_6 .4H_2O$. It is, in fact, one of the most complex ferroelectrics, from a crystallographic point of view, known so far. Its structure was determined by X-ray diffraction, and published C. A. Beevers and W. Hughes in 1941 in [83]. It contains four molecules (112 atoms) in the unit cell.

Because Rochelle salt is easily grown as large colorless single crystals, it attracted the attention of crystallographers and physicists early on. David Brewster, who studied the phenomenon of pyroelectricity (the development of electric charge by heating) on many minerals, observed this pyroelectric effect and an abnormally high pyroelectric excitation in Rochelle salt in results that he published in 1824 [84].

In 1880, Jacques and Pierre Curie discovered the phenomenon of piezoelectricity - the generation of electrical charge upon pressure application or, conversely, the development of a strain under the action of an electric field [85]. They noticed that Rochelle salt was far more piezoelectrically active than quartz and all the other crystals they had

investigated. Thomas Alva Edison was maybe the first who used its piezoelectrical effect in a commercial application in 1899 – the phonograph. However, his invention was just a curiosity and far too expensive.

In 1893, Friedrich Pockels studied the electrooptic effect - the influence of an electric field on optical properties, namely, the refraction index - in piezoelectric, noncentrosymmetric crystals, including Rochelle salt, in which he found an enhanced Kerr effect, which is known as the Pockels effect.

After some erroneous determination (well below the real value) of its dielectric permittivity, in 1893, the significance of Rochelle salt became purely academic. However, during the First World War, it merited increasing interest because of its unusually high piezoelectric moduli. The application of piezoelectrics in the generation and detection of sound waves in seawater, as a means to locate submarines, was patented in France in 1920 by Paul Langevin [86] and by Nicholson in the USA [87], [88]. Their transducers were very similar: a mosaic of thin quartz crystals glued between two steel plates (the composite having a resonant frequency of about 50 KHz), mounted in a housing suitable for submersion. Working on past the end of the war, they did achieve their goal of emitting a high frequency "chirp" underwater and measuring depth by timing the return echo. The strategic importance of their achievement was not overlooked by any industrial nation, however, and since that time the development of sonar transducers, circuits, systems, and materials has never ceased.

In the United States, J. A. Anderson at the Mount Wilson Solar Observatory in Pasadena and W. G. Cady at the Wesleyan University in Middletown reported confidentially to the National Research Council in 1918 and 1919 on the peculiarities of Rochelle salt. Independently, A. M. Nicholson at Bell Telephone Laboratories presented his extended work [89] to the joint meeting of the American Institute of Electrical Engineers and the American Physical Society in Philadelphia, also in 1919.

These results, together with various Nicholson patents, led to the development by E. W. Moore, from General Electric Laboratory, of a

solution technique by which large Rochelle salt crystals (~1 m in length) were produced for piezoelectric devices by the Brush Company. These results also initiated research on ferroelectricity in the Soviet Union in the late 1920s by P. Kobeko and I. Kurchatov and by R. D. Shulvas-Sorikina at the Physico-Technical Institute of the USSR Academy of Science in Leningrad directed by A. F. Joffe [90].

J. Valasek, who had used two crystals obtained from W. R. Whitney of General Electric Company, clearly stated in his first work [80] that the asymmetry in the charge and discharge for a capacitor with Rochelle salt as the dielectric, reported by Anderson and Cady, was due to hysteresis of the electric polarization: "*... the dielectric displacement, D, electric intensity, E, and the polarization, P, are analogous to B, H and I in the case of magnetism. Rochelle salt shows an electric hysteresis analogous to the magnetic hysteresis in the case of iron.*" The full version of his presentation was submitted to Physical Review in December 1920. It marks two milestones. Here Valasek stated for the first time that "*permanent polarisation is the natural state*" of Rochelle salt and published the first hysteresis curve of a ferroelectric material (Figure 3-1). In following papers in 1921 and 1922, Valasek presented complete charge-electric field hysteresis loops reaching saturation and a surprisingly large relative dielectric permittivity measured from -70 to 30°C, with a maximum of about 1000 at 0°C.

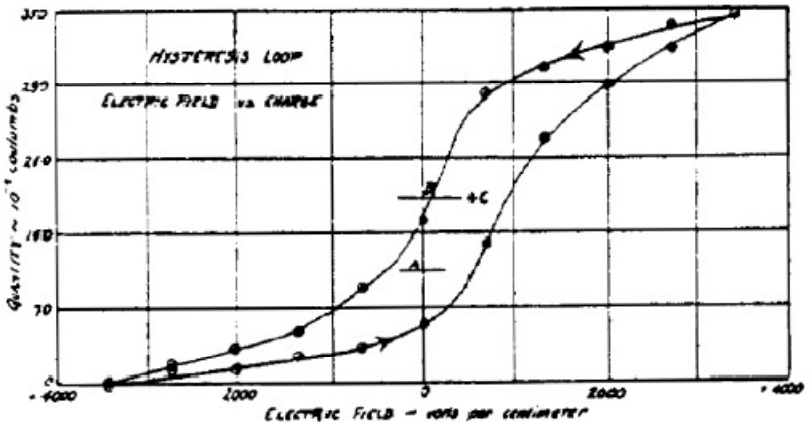

FIGURE 3-1 The first published hysteresis curve [80].

Valaseks Ph.D Thesis "Piezo-electric activity of Rochelle salt under various conditions" is dated 1922 [91]. Perhaps the most history-making graph is that of the temperature dependence of piezoelectric response, indicating the existence of a relatively narrow temperature range of high piezoelectric activity, in fact indicating the existence of two phase transitions (Figure 3-2). Indeed Valasek speaks here for the first time about the existence of two Curie points in Rochelle salt.

For more than 10 years Rochelle salt was the only recognized ferroelectric material, because acceptance of ferroelectricity as a subject worthy of more general study was slow.

Small deviations from the correct chemical composition of Rochelle salt seemed to destroy the phenomenon completely. This circumstance led to experimental problems of reproducibility and the growing conviction that the phenomenon was an accident of Nature.

Rochelle salt, together with isomorphous (Kurchatov) salts and deuterated salts, remained a subject of investigation for nearly another 20 years. Kurchatov and his collaborators revealed that in the dielectric permittivity at low field strength there were two Curie temperatures, as Valasek called them, at which sharp maxima were observed and, indeed, the ferroelectric properties of Rochelle salt manifest themselves only in a temperature interval between the two Curie points at -15 and +23°C.

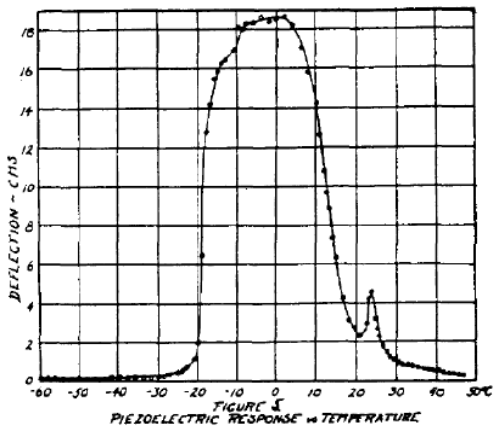

FIGURE 3-2 Piezoelectric activity of Rochelle salt vs. temperature indicates the existence of two phase transitions [91]

Kurchatov first proposed the theory that ferroelectricity is due to the orientation of the polar molecules of the water of crystallization of Rochelle salt. In addition to the work of W. R Mason at Bell Telephone Laboratories, the most remarkable contributions came from Hans Mueller, working at MIT, who, in 1940, published the first known work in which the term "ferroelectricity" was used. Without being aware of the Landau general theory of phase transitions, published in 1937, Mueller wrote an example of it with his interaction theory. This theory implied that all piezoelectric, elastic, optic, and caloric anomalies in the phenomenology of ferroelectrics can be traced back to anomalous dielectric behaviors. Thus, this concept encouraged explanations of ferroelectricity on the basis of molecular models. The work of Mueller had a great impact on researchers at the Eidgenossische Technische Hochschule (ETH) in Zurich [90].

1.2. POTASSIUM DIHYDROGEN PHOSPATE

Paul Sherrer, who followed Peter Debye as Director of the Physikalisches Institut at the ETH in 1920, also worked with Rochelle salt, and he believed that the molecules of the water of crystallization were essential for a material to be ferroelectric. In the search for new ferroelectrics, he and one of his students, Georg Busch (who found the compound), pursued a literature search for high dielectric permittivity materials. In 1935 they announced the discovery of a new ferroelectric substance with a critical temperature of about -150°C; it was potassium-dihydrogen phosphate (KH_2PO_4), which is known as KDP [79]. Ferroelectricity was no longer a singularity of Rochelle salt.

The "discovery" of KDP was followed by the isomorphous arsenate KH_2ASO_4 and the ammonium salts $NH_4H_2PO_4$ (known as ADP) and $NH_4H_2ASO_4$. The latter two salts behaved in a different way and, as late as 1952, were found by T. Nagamiya to be antiferroelectric; that is, to have antiparallel distributions of spontaneous polarization in adjacent unit cells of the crystal lattice.

Optical observations by B. Zwicker and P. Scherrer and X-ray diffraction by A. von Arx and W. Bantle were used at ETH to obtain the

first evidence (in 1944) of ferroelectric domains; that is, regions of the crystal with a given orientation of the spontaneous polarization.
ADP became the principal component of underwater transducers and submarine detectors in the Second World War, replacing the very temperature-sensitive Rochelle salt [90].
However, for frequency control applications or when the strongest possible piezoelectric effect was needed, Rochelle salt was still used. The significance of these substances was not only their usefulness as piezoelectrics, but also that they were more amenable to theoretical treatment. KDP became a model substance, because its structure, established as perovskite type by J. West in 1930, was much simpler than that of Rochelle salt.
In contrast to what was previously considered a requirement, these ferroelectrics contained no water of crystallization. They are called hydrogen bond ferroelectrics, owing to Busch's suggestion that such bonds were in the origin of their spontaneous polarization.
The same idea was applied in 1941 by John Slater, who proposed the first molecular theory of ferroelectricity based on the model of hydrogen bonds [92].

1.3. PEROVSKITE-TYPE STRUCTURE FERROELECTRICS

After the ferroelectricity of KDP was observed, another decade passed without a further, experimental breakthrough. The discovery of the ferroelectric properties of barium titanate ($BaTi0_3$) [93], the first man-made perovskite ferroelectric, independently in the United States, the United Kingdom, Russia, and Japan, was, again, a consequence of war-time research on electronics components, particularly high dielectric materials to replace mica capacitors. The high dielectric constant (ε_r=110) of rutile, Ti02, was well known, and in several laboratories there were attempts to prepare high dielectric constant ceramics.
The first inkling of unusual dielectric properties in refractory oxides amenable to ceramic preparation was recognized in a 1941 patent application by H. Thurnauer and J. Deaderick at the American Lava

Corporation, who were working on a series of barium oxide-titanium oxide compositions [94]. The material was tested at the laboratories of a customer, Erie Resistor Corporation, and found to have a high dielectric constant of 1100, ten times greater than any other ceramic known at that time.

Detailed exploration of dielectrics in titanium oxide-alkaline earth oxide systems was carried out by E. Wainer and A. N. Salomon and published in famous reports issued by the Titanium Alloy Manufacturing Company in 1942 and 1943 [95]. The result of a maximum in the dielectric permittivity versus temperature for barium titanate and a shift of this maximum to lower temperatures as strontium replaced barium was not published by Wainer until 1946. It was, however, A. von Hippel, at the Laboratory for Insulation Research at MIT, who recognized the material as a new ferroelectric (it is not clear whether Hans Mueller was involved) and summarized its properties in an article in the *Review of Modern Physics* in 1950 [96]. The discovery of ferroelectricity in BaO-TiO2 ceramics was extremely important, as it demonstrated for the first time that ferroelectricity could exist in simple oxide materials, and it was not always associated with hydrogen bonding. BaTiO3 is a member of the perovskite family named after the naturally occurring mineral perovskite CaTiO3. The simplicity of the structure of BaTiO3 (Figure 3-3) seduced several investigations to undertake X-ray diffraction studies of the structural changes occurring at the phase transitions [19] and it enabled the investigation of the most important theoretical backgrounds of these materials.

The discovery of the high dielectric constant of alkaline earth titanates at the Dubilier Condensor Co. Ltd. of London and the Steatite-Porcelain Products Co. of Stourport-on-Severn dates back to 1942, but was kept secret by war-time restrictions. An important contribution to the recognition of the new ferroelectric was made by Helen D. Megaw, who measured the spontaneous strain of the lattice associated with the spontaneous polarization by means of X-ray diffraction [97] and recognized the twinning observed below the transition temperature as a manifestation of domain formation [98].

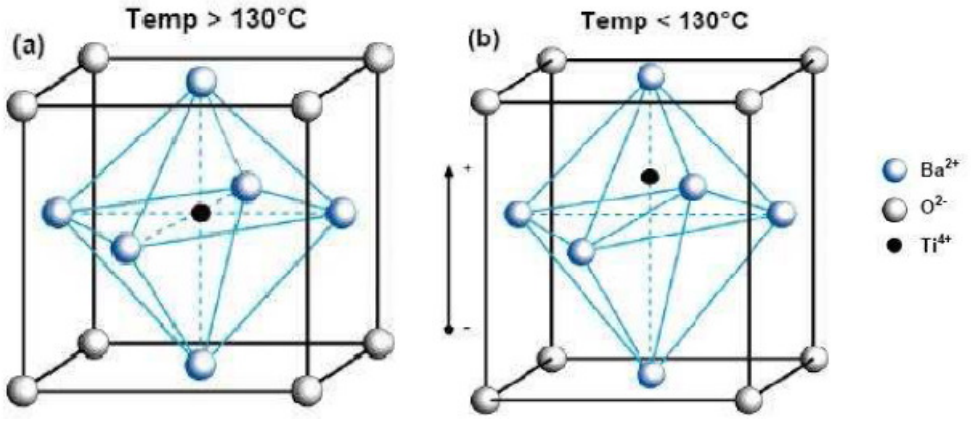

FIGURE 3-3 The BaTiO3 crystal structure above (a) and below (b) the phase transition between cubic and tetragonal.

Soon after, in works published in 1946, B. Wull and L M. Goldman noted the ferroelectric character of the material, found a dielectric Curie-Weiss law above the transition, and measured dielectric hysteresis and specific heat anomaly.

In fact, recognition of the phase transition seems to have been originally due to V. L. Ginzburg, who, knowing the Landau theory of phase transitions, suggested that $BaTiO_3$ could undergo a transition from a pyroelectric to a nonpyroelectric state. Before and during the World War II, there was some work done on Rochelle salt at the Kobayashi Institute in Tokyo [99], [100]. At this institute, S. Miyake and R. Ueda clearly recognized the discovery in 1943 by S. Waku and T. Owaga at the Electric Laboratory (NTT) of almost pure barium titanate with a room temperature dielectric permittivity of 1000 and a maximum of 4000 at the transition temperature taking place at 110°C. Miyake and Ueda's early systematic work on the new ferroelectrics was not published until 1946. These early experiments were all done with ceramic (i.e., polycrystalline) samples.

In 1946, the Zurich group, still under P. Sherrer's guidance, succeeded in growing single crystals from solution, and in 1949, H. Blattner, W. Kanzig, and W. J. Merz published a comprehensive study of $BaTiO_3$ single crystals that included crystal chemistry, dielectric and caloric behavior, domain structure, and thermodynamic relationships.

Similar efforts were made at the Laboratory for Insulation Research at MIT under the influence of B. T. Matthias from the Zurich group who was associated with the laboratory from 1946 to 1948 and then moved to Bell Telephone Laboratories, and his successor, W. J. Merz, who also subsequently joined Bell Labs in 1951.

First at the Cavendish Laboratory (due to his communications with P. Sherrer) and later at the H. H. Wills Physical Laboratory of the University of Bristol, H. F. Kay undertook a thorough study of the symmetry changes in $BaTiO_3$ and their relationship to ferroelectricity and domain structure. Kay's 1948 and 1949 papers are standard references. Nevertheless, the phenomenology of $BaTiO_3$ was still incomplete: quantitative elastic and piezoelectric data were almost nonexistent.

Most of the applications of ferroelectric materials were due to their piezoelectric properties.

Because piezoelectricity was known as a property of noncentrosymmetric crystals, the term "piezoelectric ceramic" appeared to be contradiction in itself to physicists as late as 1944. There were three basic steps in the understanding of piezoelectric ceramics and the great expansion of their use. The first was the discovery of the high dielectric constant of barium titanate, and the second was the realization that it was due to its ferroelectric character. The third significant step was the discovery of the poling process, which was established in patents by E. Wainer (1943) and R. B. Gray (1946). The poling process is the application of a sufficiently high electric field to orient the spontaneous polarization in each ceramic grain in the closest direction to that of the applied field that is allowed by the crystal structure. From the initial spherical symmetry of the unpoled ceramic, with spontaneous polarization of the grains randomly oriented, poling induces a noncentrosymmetrical, cylindrical symmetry and, therefore, ferroelectric ceramics show piezoelectricity.

Dielectric, elastic and piezoelectric properties of poled ceramics are fully characterized by knowledgement of the 3, 5 and 3 independent coefficients of the 3 x 3 , 6 x 6 and 3 x 6 , respectively, tensor coefficients defined by the constitutive equations

$$D_i = d_{ij}T_j + \varepsilon_{ij}^T E_j$$
$$S_i = s_{ij}T_j + d_{ij}E_j \tag{3.1}$$

Where D_i and E_j are the electric displacement and field components in reduced notation and S_i and T_j are the mechanical strain and stress. Superindex T indicated the coefficient at constant stress and E at constant field. The first published work on poled barium titanate ceramics appeared in 1947, authored independently by S. Roberts, who benefited from the results of von Hippel's work. The systematic of the piezoelectric effect in polarized ceramics was made by W. P. Mason in 1948, and the first set of barium titanate ceramic piezoelectric coefficients was given by H. Jaffe also in 1948.

As a result of the structural simplicity and practical use of $BaTiO_3$, that is, because it was a chemically and mechanically stable ferroelectric at room temperature and easy to prepare as ceramic or, after 1956, as a single crystal, and owing to the extraordinarily structure-sensitive character of the ferroelectricity, it was only logical to devote more effort to the search for new ferroelectrics with the same perovskite structure. Between 1949 and 1959, "the golden age of the discoveries" [101], ferroelectricity was repeatedly found in about 100 compounds. A large number of compounds were found as the result of a systematic search by Raymond Pepinsky, who was one of Valasek's most prominent graduate students in the 1930s (and later a professor at Penn State). The number of solid state ferroelectric compounds known today is about 200. The most complete list of known ferroelectrics and many relevant properties can be found in [102].

An advance of great practical importance was the discovery of the very strong and stable piezoelectric effect in lead titanate-zirconate (PZT) solid solution systems [103]. The study of the ferroelectricity of the system, from structural and electric points of view, was begun in 1951 by G. Shirane, K. Suzuki, and A. Takeda. In 1953, E. Sawaguchi published the first phase diagram. However, he did not pay attention to the piezoelectric properties, which were studied by B. Jaffe, R. S. Roth and S. Marzullo, who first published results in 1954. Extended information on this system and on piezoelectric ceramics, in general,

was collected in [103]. Since their discovery, PZT ceramics have played a major role in commercial piezoelectric applications. At the end of the war, public disclosure led to intense interest not only in academic circles, but in practical markets, in particular high capacitance, small volume capacitors in early television and radio circuits, as well as active elements for phonograph pick-ups, accelerometers, and ultrasonic generators. The British Navy, for instance, used some underwater sonar devices based on the piezoelectric response of BaTiO3 ceramics until the end of the last century. Lately, the BaTiO3 piezoelectric properties have been revisited in the form of single crystals and textured ceramics because of environmental concerns with the lead-based perovskites based on the perovskite PbZrO3-PbTiO3 system (PZT).

Later on it was discovered that one could decrease the Curie temperature (ferroelectric-paraelectric transition temperature) T_C of pure $BaTiO_3$ (T_C ~ 120 °C) down to room temperature by adding Strontium (Sr). Below the Curie temperature a ferroelectric material behaves like a "normal" ferroelectric; e.g. it has a hysteresis like Valasek observed in Rochelle Salt. But above the Curie temperature the material becomes paraelectric, the hysteresis cannot be observed anymore. From there on $Ba_{1-x}Sr_xTiO_3$ (BST) began to rock the world. The initial interest in BST thin films was due to its high dielectric constant, low dielectric loss, high dielectric breakdown and composition dependent Curie temperature enabling it to be in the paraelectric state as well as in the ferroelectric state, all of which makes it a candidate for replacing SiO_2 as charge storage dielectric for DRAMs (dynamic random access memories), MEMS-switches and varactors in phase shifters. In terms of tunability (the change of the permittivity with an applied voltage) the paraelectric state offers the opportunity for varactors (variable capacitors) and phase shifters with a linear change of the permittivity in a certain voltage region. Despite the fact that BST was (and still is) a matter of investigation for over 60 years now, there are problems with this material. First of all the leaked current is high increasing the loss (tanδ) of the film.

In recent years a new perovskite material, namely Lead Strontium Titanate, (Pb, Sr)TiO3 or PST, has attracted the interest of researchers.

Although there are health and environmental concerns with lead-based materials, this material has remarkable advantages compared to BST. It is easy to deposit crack-free via the sol-gel route, has relatively low loss and a high tunability (~ 80%), and can even be deposited on SiO2 or SiNx.

1.4. THEORETICAL TREATMENT OF FERROELECTRICITY AND TRENDS

Despite the completely-dissimilar structures of the three materials know in the middle 1940s as ferroelectrics, the existence of reversible polarization was already believed to be due to permanent dipoles undergoing order-disorder transitions at their Curie temperatures: water molecules in Rochelle salt, hydrogen bonds in KDP, and Ti ions jumping among six possible positions in $BaTiO_3$. Ferroelectricity was not a unique phenomenon.

A. F. Devonshire was at the same laboratory as the H. F. Kay group, and their experimental work on the Mueller interaction theory of Rochelle salt and its relationship to Ginzburg theory (in turn based on Landau theory) strongly stimulated their understanding of ferroelectricity and its macroscopic theory, which was published in 1951. A.F. Devonshire developed his phenomenological model of ferroelectrics on the basis of the electromechanical, structural and thermal properties of BaTiO3. This approach built upon the earlier ideas of Landau and Ginzburg and invoked the point group symmetry and nonlinear elasto-dielectric coupled interactions with electrostriction and piezoelectric coefficients. The resulting Landau-Devonshire-Ginzburg Theory (LDGT) of ferroelectrics is still the most powerful tool for the understanding of ferroelectrics. The free energy is written as a power expansion of polarization and strain, where the parameters involved are determined by associating them with measurables. The limitations in terms of basic understanding were obvious, but the possibility to include with ease changes of external constraints such as stress proved to be very valuable. The Devonshire theory [104] also made it possible to predict the value of the coercive field, which is the

threshold value of the field, below which is impossible to induce reversal of the spontaneous polarization. It was here that the theory failed completely and overestimated the value by at least 1 order of magnitude. This failure led to a research effort to understand the polarization reversal phenomena, and the concepts of domain wall nucleation and growth were explicated [105], [106].

$BaTiO_3$ was the first ferroelectric with more than one ferroelectric phase and the first to display a nonpiezoelectric, cubic centrosymmetric, prototype or paraelectric phase. Its crystal structure was of perovskite types with only five atoms per unit cell. The simplicity of the structure seduced researchers to undertake studies of the structural changes taking place at the phase transitions. An unambiguous determination of the atomic shifts came from neutron diffraction work published by the Pepinsky group [107]. This detailed knowledge was not, however, the basis of a deeper theoretical insight into the mechanisms of ferroelectricity.

The modern era of theoretical understanding arrived in terms of lattice dynamics, where the ionic motions of all constituent atoms are the basic variables that describe the displacive lattice instability at the ferroelectric transition and its effect on the dielectric response. The beginning of this era arrived with the contribution of P. W. Anderson to the Second All-Union Conference on the Physics of Dielectrics in Moscow in November 1958, which was published in 1960, and the more detailed descriptions by W. Cochran [108], who introduced the concept of "soft mode"—lattice vibration mode whose temperature dependent frequency goes to zero at the transition—to describe the ferroelectric phenomena. Soft mode allows a unified description that is unaffected by the possible complexity of any particular crystal structure and an understanding of ferroelectricity as a type of more general phenomena of structural phase transitions [79], [93], [99], [101]. Although the description of ferroelectric phase transitions of homogeneous quasi-infinite systems was solved by middle of the 1970s, new problems concerning inhomogeneous systems (for example, dipolar glasses, incommensurated phases, artificially modulated structures, or defects in electrically ordered states), purely organic materials systems,

composites, liquid crystals, and thin films, among others, arose. These problems, together with the need for deeper understanding of known concepts such as domains and the search for new and higher quality materials, driven by the demands from practical applications, define the present research efforts in the field of ferroelectrics and provide the developmental framework for piezoelectric ceramics and thin films.

1.5. GENERAL PROPERTIES OF FERROELECTRICS AND THEORETICAL CONSIDERATIONS

Ferroelectrics are known for their high dielectric constant (ε_r>1000), high tunability and the property to have a remnant polarization even in absence of an applied electric field. These features of ferroelectrics are linked and the general trend "the higher the dielectric constant, the higher the tunability" holds.

1.5.1. PIEZOELECTRICS AND SYMMETRY GROUPS

"Piezo" originates from the Greek word *piezein*, meaning to press or to squeeze. In 1880, the Curie brothers found that quartz changed its dimensions when subjected to an electric field and conversely generated an electric charge when it was pressed.

Piezoelectricity is linear interaction between mechanical and electrical systems in non-centric crystals or similar structures. The direct piezoelectric effect may be defined as the change of electric polarization proportional to the strain. A material is said to be piezoelectric if the application of an external mechanical stress gives rise to dielectric displacement in this material. This displacement manifests itself as internal electric polarization. It should be noted that the piezoelectric effect strongly depends on the symmetry of the crystal. A crystal having sufficiently low symmetry produces electric polarization under the influence of external mechanical force.

Generally, the piezoelectric effect could exist just in non-centrosymmetrical crystallographic symmetry classes. If the materials crystallographic symmetry include centre of symmetry operation, the

resulting symmetry of material subjected to such field is also centrosymmetrical. Therefore, piezoelectric effect is excluded. Centrosymmetrical crystal stays centrosymmetrical even after the application of the mechanical stress and no polar direction for the polarization vector might exist in such structure [3].

Among the 32 crystallographic classes only 21 of them are non-centrosymmetrical [109]. Moreover in cubic non-centrosymmetrical class 432, the piezoelectric coefficients are all equal zero because of symmetry. Totally, 20 "piezoelectric" crystallographic classes might exhibit non-zero piezoelectric coefficients.

All non-centrosymmetrical classes could be further divided into two groups. The first group include 10 crystallographic classes having *singular* polar axis. Crystals belonging to one of these symmetry classes are called *polar* crystals. One of the first known examples for such crystal is Tourmaline (symmetry class 3*m*). Polar crystals exhibit also pyroelectricity. Second group of non-centrosymmetrical classes include 11 classes. There are also polar symmetry axes in such symmetry classes, but they are not singular. [3]

Combinations of several crystallographically equivalent vectors directed along polar axes result in its zero sum. Materials belonging to such crystallographic classes are called *polar-neutral* crystals. Typical example of this material is α-quartz crystal with three equivalent polar directions along 2-fold symmetry axes.

In polar crystals, the piezoelectric polarization generated as a result of mechanical stress application will contribute to the spontaneous polarization existing previously. In polar-neutral crystals, the polar directions are mutually "compensated".

As a result of mechanical stress application, singular polar direction appears in such crystals. Piezoelectric polarization is generated in that direction and crystal is piezoelectrically polarized. The only exception among the polar-neutral classes is cubic 432 class, where all piezoelectric coefficients are identically equal zero because of symmetry.

Closely related is the converse (reciprocal, inverse) effect, whereby a piezoelectric crystal becomes strained if an external electric field is

applied. Both effects are the manifestation of the same fundamental property of the non-centric crystal.

Only for historical reasons the term "direct" is used about the first and not the other effect. We can study piezoelectricity using quartz crystals. A plate cut at right angles to the x-axis is called X-cut. Let its thickness be small in comparison with the other dimensions. We subject this plate to a pressure parallel with the thickness. If a compressional force (size) F is used, the polarization P_1 parallel to the thickness is proportional to the stress $T_{11} = F/A$. Hence the piezoelectric polarization charge on electrodes covering the major faces A is proportional to the force causing the strain.

If we apply tension, the sign of pressure is reversed and the sign of the electric polarization reverses too. When an electric field E is applied along the thickness of the plate the quartz plate is deformed. The deformation (the strain S_{11}) changes sign when the polarity of the field is reversed (Figure 3-4).

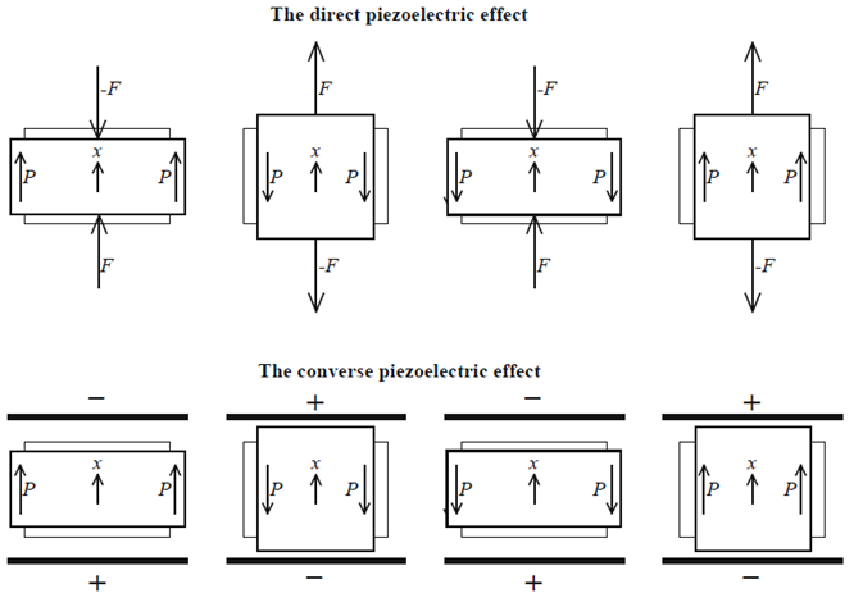

FIGURE 3-4 Direct and converse piezoelectric effects.

The direct piezoelectric effect is described by

$$P_1 = d_{111} T_{11} \tag{3.2}$$

where P_1 is the component of the polarization vector and T_{11} is the component of the stress tensor. The coefficient d_{111} is called the piezoelectric coefficient.

Conversely, if an external electric field E_1 is applied, a strain S_{11} is produced

$$S_{11} = d_{111} E_1 \tag{3.3}$$

The development of standards on piezoelectric crystals has been the product of considerable work and debate by many people. The existence of enantiomorphic crystal forms led to changes in sign conventions from time to time, as the standards committees tried to make the conventions easier to understand and use. We use the co-ordinate system adopted by the IEEE Standards [110] adopted a right-handed co-ordinate system for all crystals and quartz is not considered an exception. The crystallographic $-a$ axis is taken as X for the right quartz, whereas the $+a$ axis is taken as X for the left quartz. Extensional stress along X induces a positive charge in the direction of positive X in the right quartz, but compressional stress produces the same result in the left quartz. The sign of the piezoelectric constant is positive when a positive charge is produced in the positive direction of the axis as a result of a positive (extensional) stress. Consequently piezoelectric coefficients are positive for right quartz, and they are negative for the left quartz.

Polarization associated with a given strain is always the same, whether the strain is due to mechanical forces (direct effect) or to an impressed electric field (converse effect).

1.6. FERROELECTRICS

The class of the piezoelectric materials includes ferroelectrics. Figure 3-5 summarizes the crystallographic point groups.

Some pyroelectric materials exhibit special physical properties – so called *ferroelectric properties* – and build a special subgroup of pyroelec-

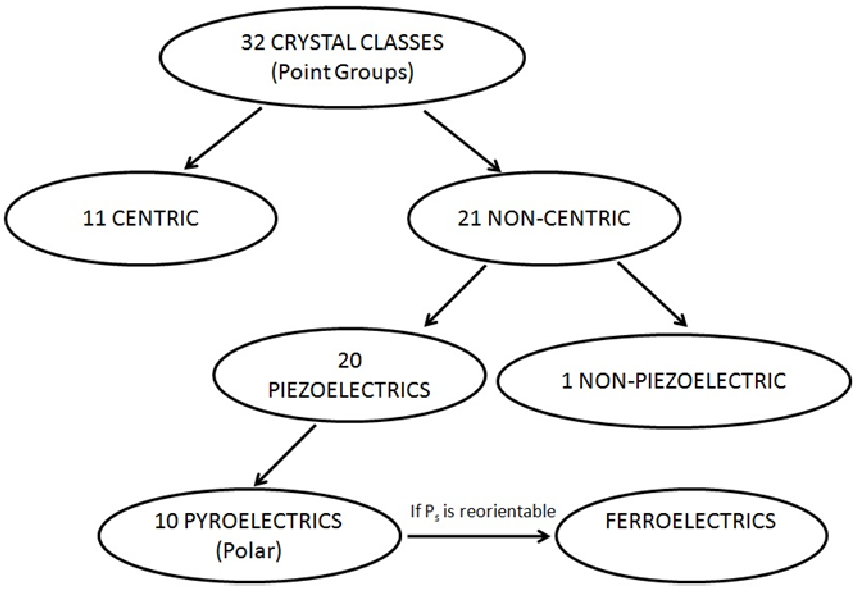

FIGURE 3-5 Point Groups classification of crystals.

tric materials, so called *ferroelectrics*.

The spontaneous polarization could be switched (reversed or rotated) from its stable orientation to the other orientation for such materials. Ferroelectric crystal could be also treated as pyroelectric crystals with switchable polarization, in that sense. Pyroelectric properties are necessary, but not sufficient conditions for the ferroelectricity.

Substantial crystal lattice reconstruction is necessary for the spontaneous polarization direction change in pyroelectric, but not ferroelectric crystal. Such lattice reconstruction could be realized only by overcoming the high energy barrier between stable atomic positions, which is rather improbable. In the ferroelectric crystal, on the contrary, the polarization direction change is realized through the very small lattice distortion and therefore it is not so energetically demanding.

The name "ferroelectricity" comes from the formal analogy between ferroelectric and ferromagnetic properties; especially between the hysteresis curves for both phenomena. Such analogy is however not valid for the related atomic-scale phenomena, which are the microstructural origin of the spontaneous polarization.

Reorientation of the spontaneous polarization is connected with the presence of so called *domain structure*. Domain is the space region with all elementary dipoles aligned in certain common direction. Dipole moment orientation might point generally in several different directions, which are energetically equivalent. Specific polarization directions for given material are governed by the symmetry of both ferroelectric and paraelectric phase (ferroelectric species). Situation is an analogy to the Weiss magnetic domains in ferromagnetic materials. The reason for the domain structure presence is the minimization of free energy of the whole crystal due to the reduction in the electric field energy. On the contrary, the crystal decomposition into domains could not proceed to the infinitely small domains because of the domain walls (i.e. the interfaces between domains) energy. Equilibrium domain structure is a result of minimization of the sum of electric field and domain wall energy. Crystals with electrically shortened outer surfaces could be theoretically expected in single domain form. Due to the defects in real crystals, the domains could appear also in such crystals.

The ferroelectric domain structure in the crystal is a reason of the non-linear behavior of the polarization as a function of an electric field. Dielectric hysteresis appears in the alternating electric fields. The dielectric hysteresis loop is one of the most important features of ferroelectric materials. Hysteresis loop or domain structure observation could serve as a proof of ferroelectricity in the material. Due to the presence of domain wall structure, the remanent polarization P_r is always smaller than the spontaneous polarization P_S.

A typical hysteresis loop describing the relationship between the resulting polarization P and the applied electric field E is shown in Figure 3-6. When the electric field is zero the ferroelectric polarization resides in one of the two stable states P_r^- and P_r^+; these are the negative and positive remnant polarizations respectively. If an external field E_{sat}^+ is applied to the ferroelectric, it is polarized to P_{sat}^+, the positive saturation polarization. After the external field is removed (i.e. $E = 0$), the polarization settles back to P_r^+. In the opposite case, with an external field E_{sat}^-, the ferroelectric is polarized to P_{sat}^-. After the field is removed, the polarization settles back to P_r^-. Thus the polarization of a

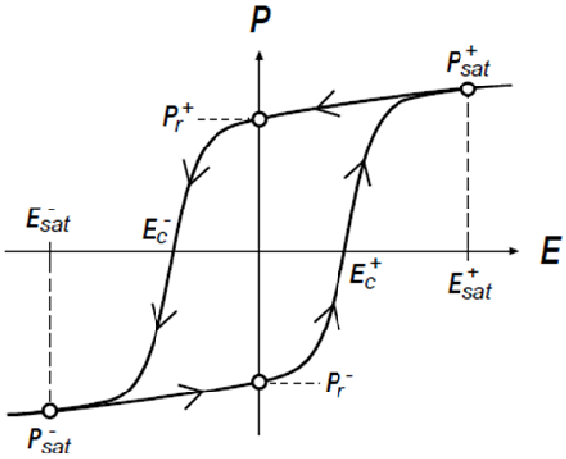

FIGURE 3-6 Ferroelectric hysteresis loop [111].

ferroelectric depends not only on the actual value of E but also on its previous values. The points where $P = 0$ are indicated as E_c^- and E_c^+; these are the negative and positive coercive fields [111]. This hysteresis loop can be observed experimentally by using a Sawyer-Tower circuit [112]. The spontaneous polarization of the material exists only in the certain temperature range. The structural change characterized by the existence of spontaneous polarization is a phase transition occurring at so called *Curie temperature* T_C. High-temperature (also called parent) phase is called paraelectric and low-temperature phase is called ferroelectric. Spontaneous electric dipole moments exist only in the ferroelectric phase, but both phases – paraelectric as well as ferroelectric – might exhibit piezoelectric properties. Most of the ferroelectric materials have only one Curie temperature, only very few crystals undergo the phase transition between ferroelectric and paraelectric phases at two different temperatures (e.g. Rochelle Salt at –18◦C and at +24◦C). The crystallographic symmetry for the ferroelectric phase is descended with respect to the paraelectric phase (group and subgroup relationship for ferroelectric species). Crystallographic symmetry of both phases is the fundamental factor for the possible spontaneous polarization orientations as well as for the domain wall structure.

Temperature range close to the phase transition temperature is the temperature region where some of the material properties exhibit anomalous behavior. Among other properties, also the strong piezoelectric effect could be observed. Paraelectric phase transfers to the ferroelectric phase by rising up the spontaneous polarization.
Similarly, reverse transition from ferroelectric to paraelectric phase might take place.

1.7. FERROELECTRIC DOMAINS

In the absence of an external force, the direction of the spontaneous polarization in an ideal ferroelectric crystal can arise with equal probability along several crystallographic directions of the prototype (paraelectric) phase. Accordingly, after the transition to a ferroelectric state the crystal breaks up into separate regions that differ in the direction of the spontaneous polarization. The regions of the crystal with uniformly oriented spontaneous polarization are called ferroelectric domains. The region between two domains is called a domain wall.
Domain walls that separate different orientations of the spontaneous polarization vector are called ferroelectric domain walls and those which separate different orientations of the spontaneous strain are called ferroelastic domain walls.
Ferroelectric domains form to minimize the electrostatic energy of the depolarizing fields and the elastic energy associated with mechanical constraints to which the ferroelectric material is subjected during the transition from the paraelectric to the ferroelectric phase.
Depolarizing fields develop whenever a nonhomogeneous distribution of the spontaneous polarization appears, for instance, during the formation of the ferroelectric phase. Also, the fall-off of the polarization at a grain boundary usually causes strong depolarizing fields of the order of 10 kV/cm. Due to these high values, the depolarizing fields cause the single-domain state of a ferroelectric to be energetically unfavorable. As a consequence, the electrostatic energy associated is minimized by splitting the ferroelectric into domains with opposite

polarization. Alternatively, the charges associated with the depolarizing fields may be neutralized by conduction of free charges through the crystal or coming from the surrounding of the material. [113]

Regarding the domain formation, Fousek and Janovec [114] have established a criterion to predict the possible domain wall orientations between two allowed polarization directions in a perfect infinite single crystal:

- During the transition to the polarized state, the crystal distorts. This distortion can be predicted from the magnitude and direction of the spontaneous polarization, and from the piezoelectric and electrostrictive coefficients in the paraelectric phase.
- Two domains having different orientations of the spontaneous polarization will have a common domain wall only along the planes for which the two distortions of the lattice match exactly. These planes are therefore possible domain walls for the crystal.

Another condition that should be fulfilled at the domain wall is the *electric neutrality*.

Unless the crystal is conductive, the normal component of the spontaneous polarization should be continuous through the domain wall; otherwise, the electrostatic energy will make it very unstable.

The domain structure that develops in single crystal perovskites is well known. The spontaneous polarization can be oriented only along three mutually perpendicular crystallographic directions (in the tetragonal phase). This gives rise to two types of domain walls: walls that separate domains with oppositely oriented polarization (called *180°-walls*), and those which separate regions with mutually perpendicular polarization (called *90°-walls*).

The 90°-walls are both ferroelectric and ferroelastic domain walls, because they separate regions with different orientation of the polarization and of the strain.

The application of the above criteria applied to tetragonal perovskites shows that the 180° domain walls can be any cylindrical surface separating regions with the spontaneous polarization parallel to the polar axis.

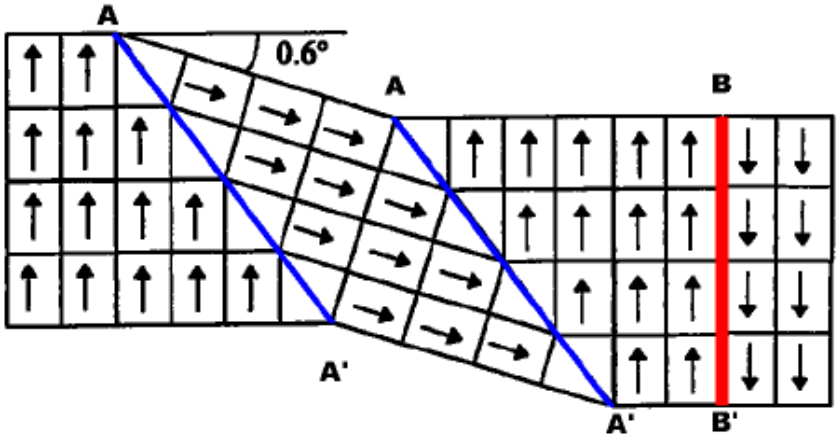

FIGURE 3-7 Ferroelectric domain walls in a perovskite ferroelectric. A-A' lines represent 90° domain walls, and the B-B' line a 180° domain wall (the tetragonality is highly exaggerated) [115].

No other restrictions are limiting their position or orientation.
The allowed 90° domain walls are parallel to the $\{110\}_{tetr}$ family of crystal planes.
The continuity of the normal component of the spontaneous polarization results in the so called head-to-tail configuration, as depicted in Figure 3-7 [115].
The ferroelectric domain structure is the most important factor that determines the ferroelectric properties of a ferroelectric material, together with domain nucleation and domain wall mobility. The way how the material splits up into domains at the formation of the ferroelectric phase depends very much on the mechanical and electrical boundary conditions imposed on the sample, as well as on the nature of the sample itself.

The domain-wall switching in a ferroelectric material, results in a ferroelectric hysteresis loop, shown again in Figure 3-8 for the sake of convenience. At small values of the ac electric field, the polarization increases linearly with the field amplitude and in this region, the field is not strong enough to switch the domains with the unfavorable direction of the polarization (AB).

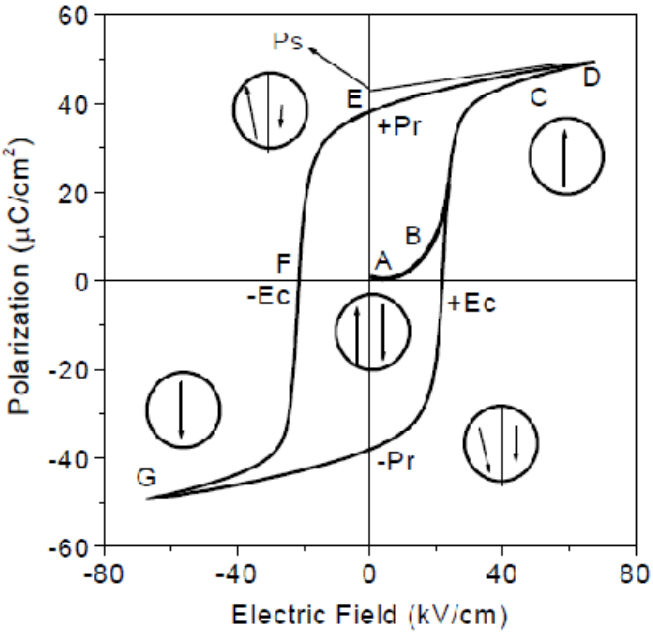

FIGURE 3-8 Polarization versus Electric field loop behavior of a ferroelectric material.

As the field is increased, the polarization of domains with an unfavorable direction of polarization starts to switch in the direction of field and rapidly increasing the measured charge density. The polarization reversal takes place by the growth of existing antiparallel domains, by domain-wall motion and by nucleation and growth of new antiparallel domain [99]. The polarization response in this region is strongly nonlinear and once all the domains are aligned, the ferroelectricity again behaves linearly (CD). With the decrease in field strength (DE), some domains back-switch, but at zero field the polarization is non-zero and to reach a zero polarization state, the field must be reversed. Further increase of the field in the negative direction (EFG) causes a new alignment of dipoles and saturation.

1.8. POLING

Poling, schematized in Figure 3-9, is a process during which a high electric field is applied on the ferroelectric ceramic samples to force the domains to reorient in the direction of the applied electric field. The poling is possible only in ferroelectric materials. Pyroelectric or piezoelectric polycrystalline materials, with randomly oriented grains cannot be poled as they lack more than one equilibrium state of the polarization vector.

Before poling, the ferroelectric ceramic does not possess any piezoelectric and pyroelectric properties owing to the random orientation of the ferroelectric domains in the ceramics. For domain reorientation, a poling field must be applied on the sample and maintained for a certain length of time. For a given field and poling time, better domain rearrangement results at higher temperature, but lower than T_C. This happens because with the increase in poling temperature, crystalline anisotropy and coercive field, E_C, of the ferroelectric materials decreases [103]. Also, with increasing temperature, space charges, which act against domain motion, decreases in ceramic materials.

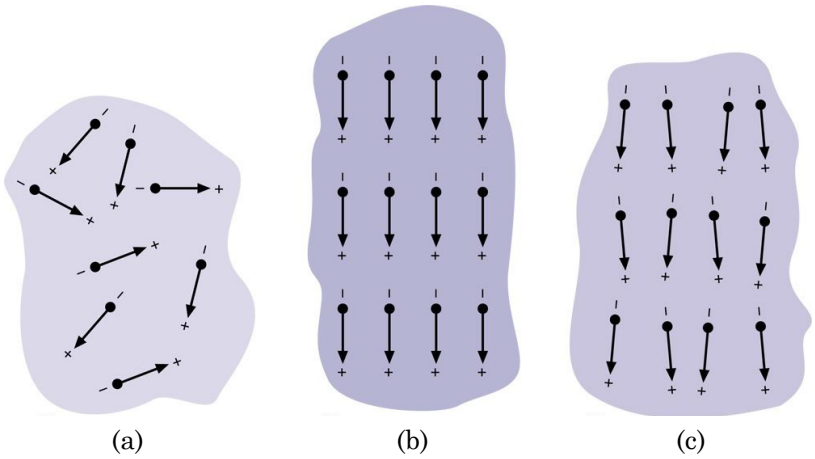

FIGURE 3-9 The poling process schematization: (a) random orientation of polar domains prior to polarization; (b) polarization DC electric field; (c) remnant polarization after electric field removed.

However, when the poling temperature is too high, problems arise as the electrical conductivity increases and the consequent increase in leakage current would result in sample breakdown during the period of poling. Sample is allowed to cool to room temperature with the field applied and field is removed at room temperature. After poling, a remnant polarization and remnant strain are maintained within the material, and it starts exhibiting piezoelectric and pyroelectric effects.

1.9. DIELECTRIC PERMITTIVITY

The origin of the high dielectric permittivity of ferroelectrics in the paraelectric phase is a delicate compensation of various kinds of atomic forces that maintains the material in a non-poled state in the absence of an electric field (see Figure 3-3a).

Because of this compensation, the restoring force opposing the poling action of the applied field is relatively weak. This results in a high dielectric permittivity of the material.

The most straightforward description of the dielectric response of ferroelectrics is given by the conventional Landau theory and is based upon an expansion of the Helmholtz free energy F with respect to the vector macroscopic polarization P. For the situation where the polarization is collinear with the macroscopic electric field E in the material, the first terms of this expansion read [116]

$$F = \frac{\alpha}{2}P^2 + \frac{\beta}{4}P^4 + \frac{\gamma}{6}P^6 - EP \tag{3.4}$$

The equilibrium configuration is determined by finding the minimum of F, where

$$\frac{\partial F}{\partial P} = 0 \tag{3.5}$$

This equation gives an expression for the electric field E as a function of the polarization P

$$E = \alpha P + \beta P^3 + \gamma P^5 \tag{3.6}$$

The linear dielectric susceptibility χ above the transition can be determined by differentiation this equation with respect to P and then setting $P = 0$ to obtain

$$\chi = \frac{P}{E} = \frac{1}{\alpha} \tag{3.7}$$

In the Landau-Devonshire theory it is assumed that around the Curie point (T~T0)

$$\alpha = \alpha_0 (T - T_0) \tag{3.8}$$

and the other coefficients in the free energy expansion are independent of temperature.

Combining the last two equations leads to the expression for the dielectric stiffness

$$\kappa = \frac{1}{\chi} = \alpha_0 (T - T_0) \tag{3.9}$$

which captures the Curie-Weiss behavior in χ observed in most ferroelectrics for $T>T_0$.

In terms of the dielectric permittivity $\varepsilon = \varepsilon_r \varepsilon_0$ with $\varepsilon_0 = 8.85 \cdot 10^{-12}\, F/m$ one can find

$$\varepsilon = \frac{C}{T - T_0} \tag{3.10}$$

where C is the Curie-Weiss constant. It should be noted here that the temperature T_0 where α changes sign is close but not exactly coincident with the Curie temperature T_C.

Including the linear temperature-dependence of α, leads to the general expression for the free energy in ferroelectrics

$$F = \frac{1}{2}\alpha_0 (T - T_0) P^2 + \frac{1}{4}\beta P^4 + \frac{1}{6}\gamma P^6 - EP \tag{3.11}$$

or for the electric field E

$$E = \alpha_0 (T - T_0) P + \beta P^3 + \gamma P^5 \tag{3.12}$$

where α_0 and γ are both positive in all ferroelectrics and β and γ describe the nonlinearity of the material.

1.10. FATIGUE, IMPRINT AND RETENTION LOSS

Three major material issues that are known to cause failure in ferroelectric devices (as memories) are fatigue, imprint and retention loss.

Fatigue is one of the most serious issues and is observed as a decrease of remnant polarization with the continuous switching between positive and negative polarization states which induce stress in the material [117]. Figure 3-10a shows the effect of fatigue observed on the hysteresis curve. The loss in remnant polarization depends on switching frequency, amplitude, temperature, etc. and may be as large as 50% or more after only 10^8 cycles for PZT with platinum (Pt) electrodes. In devices such as ferroelectric memories a loss of P_r directly translates into a loss of signal voltage and ultimately leads to the inability of the sense amplifier to discern between the two different polarization states. It has been found that the electrode material plays a crucial role in fatigue performance. For example, the recent change from Pt to IrO_2 and RuO_2 electrode material allowed extending the point where a loss of P_r starts to appear up to ~10^{12} cycles.

Another major issue, shown in Figure 3-10b is known as imprint and is described as the preference of one polarization state over the other [118]. In general, two different effects are observed. First, imprint leads to a shift of the hysteresis loop on the voltage axis, and second, to a loss of the polarization state complementary to the established one. However, it has been observed that the ferroelectric is not able to preserve the initial remnant polarization over time without loss. This loss in remnant polarization is called retention loss [119] and is shown in Figure 3-10c.

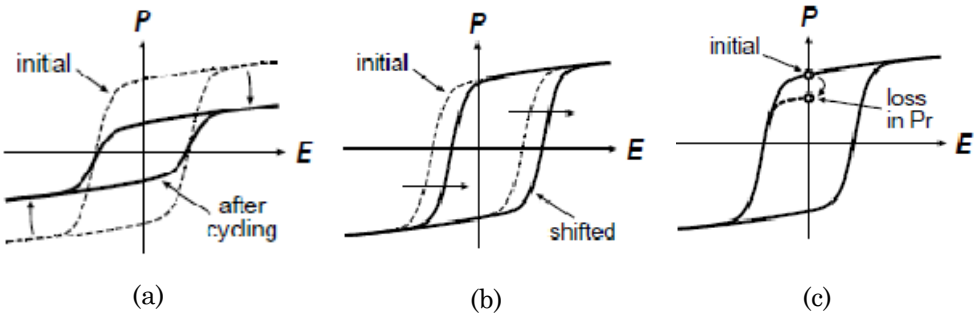

(a) (b) (c)

FIGURE 3-10 (a) Fatigue; (b) Imprint; (c) Retention loss.

2. TYPES OF FERROELECTRIC MATERIALS

There are several types of ferroelectric materials that are grouped together according to their structure. The four main types of structures include the corner sharing oxygen octahedral (perovskite type compounds), compounds containing hydrogen bonded radicals, organic polymers and ceramic polymer composites [120]. In the following a brief description of the most common ferroelectric materials is given; many others can be found in literature or surfing the web.

2.1. PEROVSKITE TYPE FERROELECTRICS

Several ferroelectric materials have structures that are closely related to perovskite, which is the name of the mineral calcium titanate (CaTiO3). The chemical formula of the perovskite family is ABO_3, where the A ions are located at the corners in a unit cell, the B ion is at the cubic center, and the O ions (oxygen ions) are at the face centers, as shown in Figure 3-11. Several useful ferroelectric oxide materials such as barium titanate (BaTiO3), lead titanate (PbTiO3), lead zirconate titanate (Pb(Zr,Ti)O3) and potassium niobate (KNbO3) have the perovskite-type structure. The perovskite family of oxides is probably the best studied family of oxides. The interest in compounds belonging to this family of crystal structures arise in the large and ever surprising variety of properties exhibited and the flexibility to accommodate almost all of the elements in the periodic system.

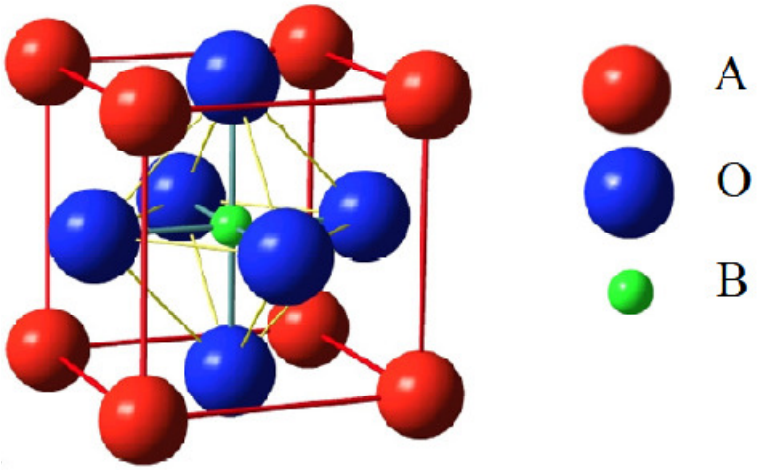

FIGURE 3-11 Schematic diagram of the ABO_3 perovskite structure.

2.2. BARIUM TITANATE ($BaTiO_3$)

Barium titanate, having the chemical formula $BaTiO_3$, is a white powder and transparent as larger crystals. This titanate is a ferroelectric ceramic material, with a photorefractive effect and piezoelectric properties. The solid can exist in four phases, listing from high temperature to low temperature: cubic, tetragonal, orthorhombic, and rhombohedral crystal structure. All of the phases exhibit the ferroelectric effect except the cubic phase. The crystallographic dimensions of the barium titanate lattice change with temperature, as shown in Figure 3-12, due to distortion of the TiO_6 octahedra as the temperature is lowered from the high temperature cubic form [121].

All transitions are of the first order and the temperature dependence of the dielectric constant shows discontinuities at the transitions and peak values as high as 10^4 as shown in Figure 3-13. Above T_c = 120°C the dielectric constant follows the Curie-Weiss law; the ceramic is cubic structure acting isotropic. The Ti atoms are all in equilibrium positions in the center of their octahedra. Shifting of Ti atom due to applied electric fields could cause the structure to be altered, creating electric dipoles.

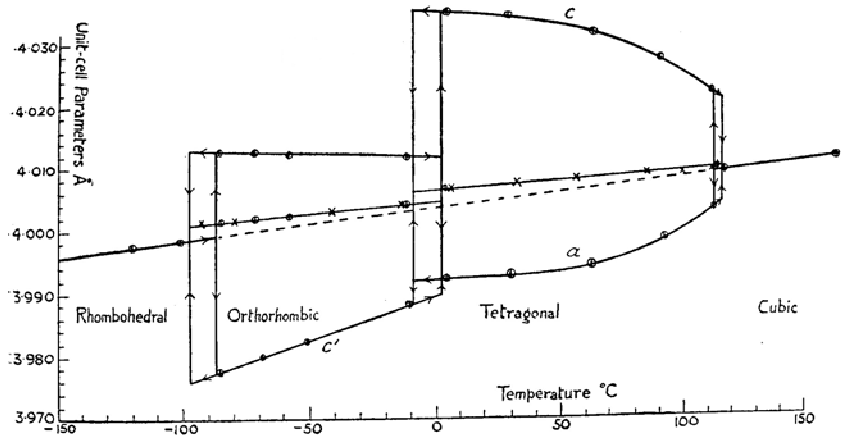

FIGURE 3-12 Lattice parameters of $BaTiO_3$ as a function of temperature.

For example, when temperature is below the Curie temperature, the octahedral structure changes from cubic to tetrahedral symmetry and the position of the titanium ion becomes an off-center position corresponding to a permanent electrical dipole. As the temperature is changed, the crystallographic dimensions change due to distortion of the octahedra resulting in octahedra being coupled together and having a very large spontaneous polarization that leads to a large dielectric constant. These sensitive crystallographic fluctuations with the temperature are shown in Figure 3-14.

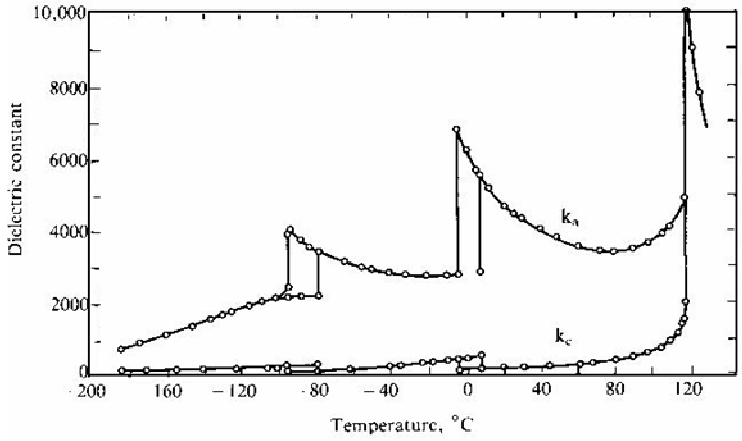

FIGURE 3-13 Dielectric constants of BaTiO3 as a function of temperature.

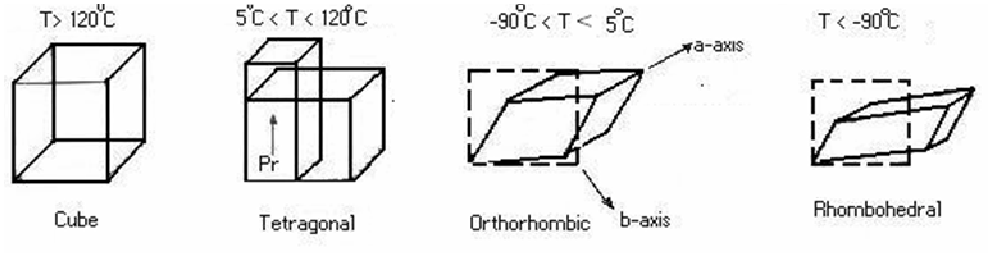

FIGURE 3-14 Crystallographic changes of $BaTiO_3$.

The dielectric characteristics of barium titanate ceramics with respect to temperature, electric field strength, frequency and time (aging) are also very dependent on the substitution of minor amounts of other ions, on microstructure, and in particular on fine grain size. For example, the room-temperature relative dielectric constant increases as the grain size of the fast-fired $BaTiO_3$ ceramic is decreased [122]. When compared with milling method, chemical mixing techniques show an advantage in enhancing the microhomogeneity of additives, modifying the surface states and then have an effect on the properties of coated ceramics. For instance, in coating process silica is a well-known sintering aid that improves the sintering behavior of $BaTiO_3$ particles and also can produce a core-shell-like structure. By adjusting the core-shell structure, we can control the dielectric properties. The coating process not only can increase the shrinkage rate that improves the sintering behavior but also can inhibits the grain growth.
Barium titanate is largely used in multilayer ceramic capacitors and in positive temperature coefficient (PTC) thermistors.

2.3. POTASSIUM NIOBATE ($KNbO_3$)

$KNbO_3$ is in many ways qualitatively similar to barium titanate. It undergoes the same series of ferroelectric transitions in the same sequence as the temperature is lowered. The cubic-tetragonal transition is at T=435°C, the tetragonal-orthorhombic at 225°C and the orthorhombic-rhombohedral at -10°C. As in $BaTiO_3$ the transitions are all of first order and hysteresis effects are readily observed.

2.4. LEAD TITANATE ($PbTiO_3$)

Lead titanate is a ferroelectric perovskite-type material with a low dielectric constant and a high Curie temperature, T_C = 490°C at which the phase transition from the cubic paraelectric phase (above Curie temperature) to the tetragonal ferroelectric phase (below Curie temperature) occurs. When cooled to below the Curie temperature, high-purity, dense $PbTiO_3$ ceramics breaks into powder. For this reason in earlier studies lead titanate ceramics were prepared modifying $PbTiO_3$ with small amounts of different additives (as MnO_2) [123].
Its properties make it attractive for high-temperature and high frequency transducer applications. These applications include surface acoustic wave (SAW) devices, actuators and piezoelectric transducer [124]. It is a good ferroelectric for infra-red (IR) detectors, high frequency filters and opto-electronic devices. Ferroelectric lead titanate thin films, grown directly on a semiconductor such as Si, form a very promising combination for nonvolatile memory devices as well as piezoelectric and pyroelectric sensor applications [125].

2.5. LEAD ZIRCONATE ($PbZrO_3$)

$PbZrO_3$ is a well-known perovskite which shows an antiferroelectric behavior. At high temperatures it possesses the prototype cubic perovskite structures but on decrease of temperature it exhibits a marked dielectric anomaly at about 230°C. The high-temperature phase is paraelectric with the dielectric constant following a Curie-Weiss law with Curie constant $C \approx 1.6\times10^{-5}\,K$ and a Weiss temperature T_0 = 190°C. Although the general character of this dielectric anomaly appears similar to that in a typical first-order ferroelectric perovskite like $BaTiO_3$, dielectric hysteresis is not generally observed in low-temperature phase and X-ray and neutron diffraction experiments have established that the room-temperature structure is antiferroelectric.
Early experiments on ceramic samples of $PbZrO_3$ indicated that phase transition at 230°C was the only structural transition to occur as a function of temperature in zero field, but that application of an external electric field below T_c induced a transition to a rhombohedral

ferroelectric phase. This implied that the antiferroelectric and ferroelectric phases were very closely equal in free energy. However, recent works on high-purity ceramic and single-crystal specimens have shown it is possible that the rhombohedral ferroelectric phase may actually be stable in zero field within a narrow temperature range between the antiferroelectric and paraelectric phases. The interposed ferroelectric phase has been observed to be stable over a temperature range of order 10-25 degC below T_c=230°C but the range of stability depends very sensibility upon stoichiometry and growth conditions of the samples.

2.6. LEAD ZIRCONATE TITANATE (PZT)

The $Pb(Zr,Ti)O_3$, typically indicated as PZT, is a solid solution of $PbZrO_3$ and $PbTiO_3$. At room temperature, $PbZrO_3$ is in an orthorhombic antiferroelectric phase in which the spontaneous polarization is antiparallel in neighboring unit cells. $PbTiO_3$ at room temperature is in a tetragonal ferroelectric phase in which the spontaneous polarization is parallel in neighboring unit cells. PZT has the ABO_3 type perovskite structure with Ti^{4+} ions and Zr^{4+} ions occupying B-sites randomly.

The phase diagram of PZT solid solution is shown in Figure 3-15a. The structure of PZT, at high temperature, is a cubic paraelectric phase. Below T_c, PZT has the ferroelectric or antiferroelectric phase. A tetragonal ferroelectric phase (the Ti rich region of the phase diagram) and a rhombohedral ferroelectric phase (the Zr rich region) are divided by the morphotropic phase boundary (MPB). The composition of Ti:Zr of the MPB is 52:48 at room temperature. Near the composition corresponding to the MPB, there is an abrupt change in lattice constants of PZT as shown in Figure 3-15b. Since the tetragonal and the rhombohedral phases coexist at the MPB [126], large piezoelectric coefficients, dielectric permittivity, and remnant polarization can be observed in this region [127]. The anomalous properties near the MPB can be explained by a phase transition between the tetragonal and rhombohedral phases [128].

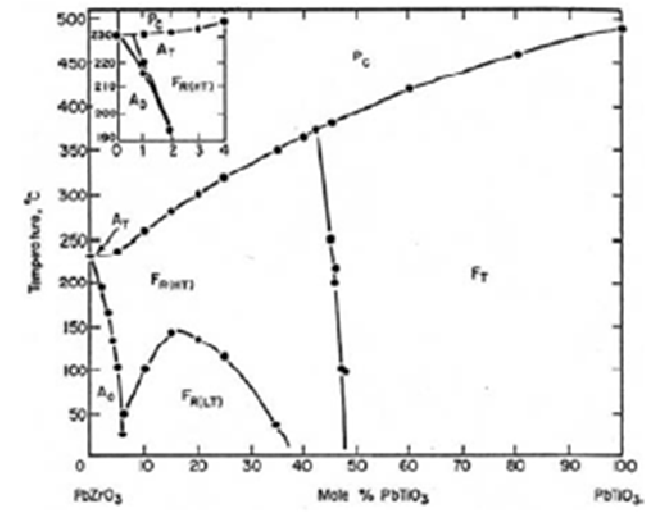

(a)

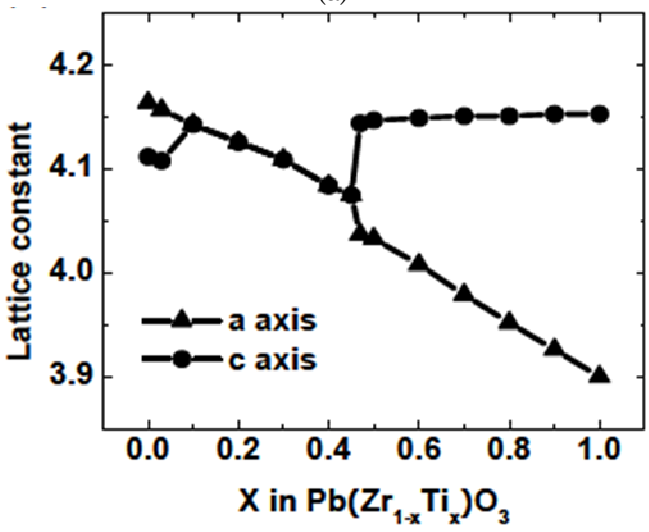

(b)

FIGURE 3-15 (a) Phase diagram and (b) lattice constants of $Pb(Zr,Ti)O_3$ solid solution.

The material features an extremely large dielectric constant at the morphotropic phase boundary (MPB). These properties make PZT-based compounds one of the most prominent and useful electroceramics. Commercially, it is usually not used in its pure form, rather it is doped

with either acceptor dopants, which create oxygen (anion) vacancies, or donor dopants, which create metal (cation) vacancies and facilitate domain wall motion in the material. In general, acceptor doping creates hard PZT while donor doping creates soft PZT. Hard and soft PZT's generally differ in their piezoelectric constants. Piezoelectric constants are proportional to the polarization or to the electrical field generated per unit of mechanical stress, or alternatively is the mechanical strain produced by per unit of electric field applied. In general, soft PZT has a higher piezoelectric constant, but larger losses in the material due to internal friction. In hard PZT, domain wall motion is pinned by the impurities thereby lowering the losses in the material, but at the expense of a reduced piezoelectric constant.
PZT is used to make ultrasound transducers and other sensors and actuators, as well as high-value ceramic capacitors and FRAM chips. PZT is also used in the manufacture of ceramic resonators for reference timing in electronic circuitry.

2.7. LEAD LANTHANUM ZIRCONATE TITANATE (PLZT)

This is a transparent ceramic, whose general formula is $(Pb_{1-x}La_x)(Zr_{1-y}Ti_y)_{1-x}O_3$ obtained doping the PZT with La^{3+} ions. The structure is very similar to that of $BaTiO_3$ and PZT but its feature of transparency makes it suitable for electro-optical applications. Figure 3-16 shows the phase diagram of PLZT as a function of temperature and composition. We note the presence of ferroelectric phases with tetragonal (FE_{tet}) and rhomboid (FE_{Rb}) structure, a ferroelectric relaxor-type phase with cubic structure (SFEc), an antiferroelectric phase with orthorhombic structure (AFE) and a paraelectric phase with cubic structure (PE_{cubic}).

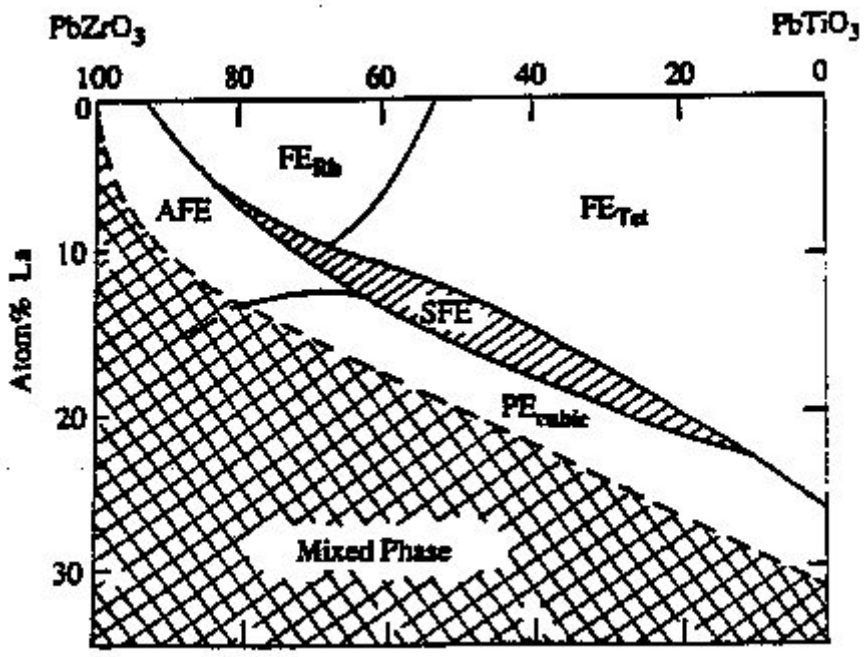

FIGURE 3-16 Phase-Temperature diagram of PLZT as a function of %La.

2.8. LITHIUM NIOBATE ($LiNbO_3$)AND LITHIUM TANTALATE ($LiTaO_3$)

Lithium niobate and Lithium tantalate have been the object of intensive study because of their large optic non-linearities. $LiNbO_3$ is a compound of niobium, lithium, and oxygen. Its single crystals are an important material for optical waveguides, mobile phones, optical modulators and various other linear and non-linear optical applications.

Lithium niobate is a colorless solid insoluble in water. It has trigonal crystal system, which lacks inversion symmetry and displays ferroelectricity, Pockels effect, piezoelectric effect, photoelasticity and nonlinear optical polarizability. Lithium niobate has negative uniaxial birefringence which depends slightly on the stoichiometry of the crystal and on temperature. It is transparent for wavelengths between 350 and 5200 nanometers.

Lithium niobate can be doped by magnesium oxide, which increases its resistance to optical damage (also known as photorefractive damage) when doped above the optical damage threshold. Other available dopants are Fe, Zn, Hf, Cu, Gd, Er, Y, Mn and B.

Lithium niobate is used extensively in the telecoms market, e.g. in mobile telephones and optical modulators. It is the material of choice for the manufacture of surface acoustic wave devices. Other uses are in laser frequency doubling, nonlinear optics, Pockels cells, optical parametric oscillators, Q-switching devices for lasers, other acousto-optic devices, optical switches for gigahertz frequencies, etc. $LiTaO_3$ is a crystalline solid which possesses unique optical, piezoelectric and pyroelectric properties which make it valuable for nonlinear optics, passive infrared sensors such as motion detectors, terahertz generation and detection, surface acoustic wave applications, cell phones and possibly pyroelectric nuclear fusion.

Both compounds are ferroelectric at room temperature and may be grown in the form of large optic-quality single crystals. They are uniaxials at all temperatures, with only a single structural phase transition (paraelectric-ferroelectric) and exhibit second-order (or close) phase transitions but their Curie temperature are very high (620°C for $LiTaO_3$ and ≈1200°C for $LiNbO_3$) placing the region of most intense structural activity in an inconvenient temperature region, particularly for niobate which melts only about 50degC above its Curie point [99].

2.9. FERROELECTRIC RELAXORS

A large number of perovskites containing lead show abnormal characteristics due to a strong frequency and temperature dependence of the permittivity. These materials are called relaxors. In particular, the maximum constant dielectric shifts to higher temperatures with increasing frequency. Examples are lead zinc niobate $Pb(Zn_{1/3}Nb_{2/3})O_3$ or PZN, and lead magnesium niobate $Pb(Mg_{1/3}Nb_{2/3})O_3$, better known by the acronym PMN. It is believed that they consist of weakly-interacting mesoscopic ferroelectric regions, rather than the usual ferroelectric domains.

TABLE 3-1 Differences between normal and relaxor ferroelectrics.

Property	Normal Ferroelectric	Relaxor Ferroelectric
Dielectric temperature dependence	Sharp 1st or 2nd order transition at Curie point T_c	Broad diffused phase transition at Curie maxima
Dielectric frequency dependence	Weak Frequency dependence	Strong frequency dependence
Dielectric behavior in paraelectric range ($T > T_c$)	Follows Curie-Weiss law	Follows Curie-Weiss square law
Remnant polarization	Strong P_r	Weak P_r
Scattering of light	Strong anisotropy	Very weak anisotropy to light
Diffraction of X-Rays	Line splitting due to deformation from paraelectric to ferroelectric phase	No X-Ray line splitting

These features make them interesting because show many useful properties:

- Very high permittivity in a wide temperature range
- High electrostrictive strain
- Strong piezoelectric, pyroelectric, and electro-optical response, when subjected to a constant electric field.

Table 3-1 shows the main differences between relaxor and normal ferroelectrics.

2.10. FERROELECTRIC POLYMERS. THE PVDF

The ferroelectricity is also present in many polymers [129]. Ferroelectric polymers have low piezoelectric coefficients and low permittivity, on the other hand they are light, have good acoustic impedance and are suitable for organic and biological applications.

Ferroelectric polymers, such as polyvinylidene fluoride (PVDF) and poly[(vinylidenefluoride-co-trifluoroethylene] [P(VDF-TrFE)], are very

attractive for many applications because they exhibit good piezoelectric and pyroelectric responses and low acoustic impedance, which matches water and human skin. More importantly, they can be tailored to meet various requirements. A common approach for enhancing the dielectric constant is to disperse a high-dielectric-constant ceramic powder into the polymers. Popular ceramic powders are lead based complexes such as $PbTiO_3$ and $Pb(Zr,Ti)O_3$. This can be disadvantageous because lead can be potentially harmful and at high particulate loading, the polymers lose their flexibility and a low quality composite is obtained. Current advances use a blending procedure to make composites that are based on the simple combination of PVDF and cheap metal powders. Specifically, Ni powders were used to make up the composites. The dielectric constants were enhanced from values there were less than 10 to approximately 400. These ferroelectric materials have also been used as sensors. More specifically, these types of polymers have been used for high pressure and shock compression sensors [130]. It has been discovered that ferroelectric polymers exhibit piezoluminescence upon the application of stress. Piezoluminescence has been looked for in materials that are piezoelectric.

PVDF is a highly non-reactive and pure thermoplastic fluoropolymer. It is a specialty plastic material used generally in applications requiring the highest purity, strength, and resistance to solvents, acids, bases and heat and low smoke generation during a fire event. Compared to other fluoropolymers, it has an easier melt process because of its relatively low melting point of around 177°C. It can be injected, molded or welded and is commonly used in the chemical, semiconductor, medical and defense industries, as well as in lithium ion batteries.

2.11. SEMICONDUCTOR FERROELECTRICS

The existence of ferroelectric properties in semiconductors is known since ‘50 [131]. Recently has been discovered the existence of a series of IV-VI compounds which are not only narrow-band gap semiconductors but also exhibit perhaps the simplest ferroelectric lattice instability yet studied. These materials, of which germanium telluride (GeTe) and tin

telluride (SnTe) are the most studied, are examples of diatomic ferroelectrics, which are the simplest conceivable class of ferroelectrics, with the order parameter involving simply a relative displacement of the only two atoms in the unit cell.
The Curie temperature T_c for GeTe is about 670 K while that of SnTe is much smaller $T_c \approx 100$ K. The system GeTe-SnTe also forms a complete solid solution with T_c falling smoothly and almost linearly with increasing tin content. [99]

3. APPLICATIONS OF FERROELECTRICS

Throughout its history the study of ferroelectriciy has been closely linked with device applications. Since the discovery of the Rochelle salt ferroelectrics materials have been largely used as piezoelectrics in a huge number of applications. However, piezoelectric applications will not be covered here because they do not directly involve the ferroelectric nature of the material and are largely discussed in literature [3], [132].
Many ferroelectrics were discovered during bursts of activity as concepts for new devices evolved for which ferroelectrics seemed suited. $BaTiO_3$ was accidentally discovered during a search for high-dielectric-constant materials for capacitors. Later came the search for computer memory elements and the bistable polarization of ferroelectrics made them attractive candidates for binary memories. The memory is non-valatile and does not require a holding voltage. To record information the polarization may be reversed or reoriented by application of an electric field greater than the coercive field. For erasure the polarization can be returned to its original state with an applied field of opposite polarity. To read the information there is a wide range of possibilities which may be divided into two broad classifications: those in which the stored information is retrieved by electrical means, and those in which it is retrieved by optical means via an electro-optic effect.
The next burst of activity came in the mid-1960's when it was realized that the large nonlinear polarizability of ferroelectrics makes them one of the most promising classes of materials for electro-optical and optical parametric devices. The electro-optic properties can be also used as the basis for digital and storage display devices. Another important

application of ferroelectric is for the modulation of light. Such modulators are required for most optical communications systems where the high-frequency laser carrier allows large-information bandwidths to be transmitted with complete isolation from electrical interference. Ceramics have for a long time been of interest for dielectric and piezoelectric applications but with the development of optically transparent ceramics they arose interest because they offer a wide range of possible electro-optic applications in pothonics and optoelectronics including several which involve polarization reversal. The advantages of ceramics in terms of ease of preparation and cost and of the variety of compositions and properties are obvious.

One of the earliest applications is Ferpic (Ferroelectric Picture Memory Device) [133], a sandwich structure consisting of transparent electrodes, a photoconductive film and a thin plate of fine-grained ferroelectric ceramic. Initally the ceramic plate is uniformly DC-poled laterally, then, storage is achieved by switching domains at points corresponding to the image's high-intensity regions. To switch domains, a high-contrast transparency is placed in front of the Ferpic and illuminated, creating low-impedance regions in the photoconductive film. Viewing/reading the memorized image is accomplished by passing polarized light through the Ferpic and an analyzer. When the polarizer and the analyzer are parallel, the regions with remnant polarization normal to the plate produce a bright image, and the other regions produce a dark image. Sandia National Laboratories designed PLZT goggles for the U.S. Air Force to provide thermal and flashblindness protection for aircraft personnel [134].

PLZT eye glasses for stereo TV have been fabricated using the light shutter principle [135]. The lenses consist of a pair of optically isotropic PLZT discs sandwiched between two crossed polarizers. When zero voltage is present between the electrodes, light will not be transmitted. The transmitted light intensity increases with increasing applied voltage, and reaches a maximum when a phase difference (ritardation) of 180° is induced in the PLZT disc (at the half-wave voltage). Stereo TV images of an object are taken by two video cameras corresponding to the two eyes and the signal from each camera is mixed alternately to make

a frame for the right and left eyes. When viewing, the right and left PLZT shutters are triggered synchronously to each image frame, resulting in a stereo image.

During the ups and downs of the development of ferroelectrics for memories and optical devices the development of pyroelectrics as thermal detectors of infrared radiation has been steadily increasing because they have a useful combination of attributes as a broad spectral response and room-temperature operation. Thermal detectors pyroelectrics may be used to detect any radiation which results in a temperature change of the crystal, i.e. X-rays to microwaves and even particles. They also have the useful features of simplicity of construction and operation and do not require an external bias field. However, in contrast with other thermal detectors, the pyroelectric current response depends on the rate of change of temperature rather than temperature itself so they are much higher-frequency device than other thermal detectors. Pyroelectrics detectors can also be used to record infrared images.

Many others applications have been proposed and are currently under studies. In previous sections some applications such as multi-layer capacitors and PTC thermistors have been mentioned. There are several directions for ferroelectrics research: substrate-film interfaces and high-strain states, finite size effects, nanotubes and nanowires, electrocaloric devices, ferroelectric random access memories (FeRAMs), dynamic random access memory (DRAM) capacitors, electron emitters, weak–magnetic field sensors, magnetoelectrics, and self-assembly. Ferroelectric liquid crystals (smectic thin films) probably have a more mature commercial product line (spatial light modulators and video camera view-finders) [136].